



For peer review only. Do not cite.

**Mass Extinction, Gradual Cooling, or Rapid Radiation?
Reconstructing the Spatiotemporal Evolution of the Ancient
Angiosperm Genus *Hedyosmum* (Chloranthaceae) Using
Empirical and Simulated Approaches**

Journal:	<i>Systematic Biology</i>
Manuscript ID:	USYB-2009-224.R2
Manuscript Type:	Regular Manuscript
Date Submitted by the Author:	20-Feb-2011
Complete List of Authors:	Antonelli, Alexandre; University of Gothenburg, Plant and Environmental Sciences Sanmartín, Isabel; Real Jardín Botánico-CSIC, Department of Biodiversity and Conservation
Keywords:	Chloranthaceae, <i>Hedyosmum</i> , biogeography, Neotropics, diversification, Andean uplift, high extinction, incomplete taxon sampling

SCHOLARONE™
Manuscripts

Only

1
2
3
4 1 ARTICLE SUBMISSION TO SYSTEMATIC BIOLOGY5
6
7
8 2 TITLE PAGE9
10
11 3 *Running head:* SPATIOTEMPORAL EVOLUTION OF *HEDYOSMUM*12
13
14 4 *Title:* Mass Extinction, Gradual Cooling, or Rapid Radiation? Reconstructing the15
16 5 Spatiotemporal Evolution of the Ancient Angiosperm Genus *Hedyosmum* (Chloranthaceae)17
18 6 Using Empirical and Simulated Approaches19
20
21
22 7 *Authors:* Alexandre Antonelli^{1*}, Isabel Sanmartín^{2*}23
24
25 8 ¹*Gothenburg Botanical Garden, Carl Skottsbergs gata 22A, 413 19 Göteborg, Sweden &*
26
27 9 *University of Gothenburg, Department of Plant and Environmental Sciences, Carl*
28 10 *Skottsbergs gata 22B, 413 19 Göteborg, Sweden. E-mail: alexandre.antonelli@vregion.se.*
29 11 *Phone: + 46 31 741 1115*30
31 12 ²*Real Jardín Botánico, CSIC; Plaza Murillo 2, 28014, Madrid, Spain. E-mail:*32
33 13 *isanmartín@rjb.csic.es. Phone: +34 (91) 420 30 17. Fax: +34 (91) 420 01 57*34
35
36
37 14 * The two authors have contributed equally to the paper. Both are corresponding authors.
38
39
40
41
42
43
44
45
46
47
48
49
50
51
52
53
54
55
56
57
58
59
60

15 ABSTRACT

16 Chloranthaceae is a small family of flowering plants (65 species) with an extensive fossil
17 record extending back to the Early Cretaceous. Within Chloranthaceae, *Hedyosmum* is
18 remarkable because of its disjunct distribution – one species in the Paleotropics and 44
19 confined to the Neotropics – and a long “temporal gap” between its stem age (Early
20 Cretaceous) and the beginning of the extant radiation (late Cenozoic). Is this gap real,
21 reflecting low diversification and a recent radiation, or the signature of extinction? Here we
22 use paleontological data, relaxed clock molecular dating, diversification analyses, and
23 parametric ancestral area reconstruction to investigate the timing, tempo, and mode of
24 diversification in *Hedyosmum*. Our results, based on analyses of plastid and nuclear
25 sequences for 40 species, suggest that the ancestor of Chloranthaceae and the *Hedyosmum*
26 stem lineages were widespread in the Holarctic in the Late Cretaceous. High extinction rates,
27 possibly associated with Cenozoic climatic fluctuations, may have been responsible for the
28 low extant diversity of the family. Crown group *Hedyosmum* originated c. 36 – 43 Ma and
29 colonized South America from the north during the Early-Middle Miocene (c. 20 Ma). This
30 coincided with an increase in diversification rates, probably triggered by the uplift of the
31 northern Andes from the Mid-Miocene onwards. This study illustrates the advantages of
32 combining paleontological, phylogenetic, and biogeographic data to reconstruct the
33 spatiotemporal evolution of an ancient lineage, for which the extant diversity is only a
34 remnant of past radiations. It also shows the difficulties of inferring patterns of lineage
35 diversification when incomplete taxon sampling is combined with high extinction rates.

36 KEY WORDS

37 Chloranthaceae, *Hedyosmum*, biogeography, Neotropics, diversification, Andean uplift, high
38 extinction, incomplete taxon sampling.

1
2
3 39 Interest in inferring the geographic origin and temporal diversification of organisms has
4
5 40 increased in the last decades. Where and when did a lineage originate? Under which
6
7
8 41 ecological and climatic conditions did it evolve? With the advent of molecular phylogenetics,
9
10 42 we can now address questions concerning patterns of species diversification across both time
11
12 43 and space. Advances in the fields of molecular dating and historical biogeography can be
13
14
15 44 combined to provide clues on ancestral areas and divergence times (Drummond et al. 2006;
16
17 45 Drummond and Rambaut 2007; Ree and Sanmartín 2009) and to examine the putative
18
19 46 correlation between range evolution, lineage diversification, and the appearance of key
20
21 47 adaptations or adaptive radiations (Moore and Donoghue 2007).

22
23
24 48 At the same time, the increasing availability of molecular phylogenies and associated
25
26 49 divergence times has spurred the development of new methods to estimate rates of speciation
27
28 50 and extinction from phylogenetic data of extant species (Nee et al. 1992, 1994a,b; Paradis et
29
30 51 al. 2004; Rabosky 2006a) and to detect changes in diversification rate through time and
31
32 52 across lineages (Pybus and Harvey 2000; Harmon et al. 2003; Rabosky 2006b; Weir 2006;
33
34 53 Rabosky and Lovette 2008; Alfaro et al. 2009). Here, we address the effect of the interplay
35
36 54 between range evolution, adaptive radiation, and extinction on the tempo and timing of
37
38 55 lineage diversification in the ancient angiosperm family Chloranthaceae, with special focus
39
40 56 on its most species-rich genus, *Hedyosmum*.

41
42 57 Chloranthaceae is a small family of flowering plants (c. 65-70 species) with an
43
44 58 extensive fossil record extending back to the Early Cretaceous (Eklund et al. 2004). It
45
46 59 comprises four genera that are disjunctly distributed in the Old and New Worlds:
47
48 60 *Chloranthus* (10 species), *Sarcandra* (2 sp.), and *Ascarina* (20 sp.) are confined to the
49
50 61 Paleotropics, including east Asia (*Chloranthus* and *Sarcandra*) and Australasia (*Ascarina*),
51
52 62 while *Hedyosmum* (about 45 sp.) occurs in Central and South America and the West Indies
53
54
55
56
57
58
59
60

63 (see Appendix S1 available at <http://www.sysbio.oxfordjournals.org>), with a single species in
64 southeastern Asia (*H. orientale*).

65 Because of its early diverging position in the angiosperm tree and its extensive and deep
66 fossil record extending back to the Early Cretaceous, the Chloranthaceae have played a
67 prominent role in understanding the origin and early diversification of angiosperms (Eklund
68 et al. 2004). In fact, the family possesses one of the oldest and most abundant fossil records
69 among angiosperms (Eklund et al. 2004). *Clavatipollenites* fossil pollen, associated with the
70 stem lineage of Chloranthaceae, and *Asteropollis* pollen, attributed to stem *Hedyosmum*, have
71 been found in a worldwide range of localities from the Early Albian (Early Cretaceous: ~110
72 Ma), indicating that the family once had a more cosmopolitan distribution covering both
73 Laurasian and Gondwanan landmasses (Eklund et al. 2004).

74 The phylogenetic position of the family has been subject to much debate over the past 50
75 years (for a review, see Endress and Doyle 2009). In comparison, intra-familial relationships
76 within Chloranthaceae have received less attention. Both morphological (Doyle and Endress
77 2000; Doyle et al. 2003; Eklund et al. 2004) and molecular analyses (Qiu et al. 2000; Zanis et
78 al. 2002; Zhang and Renner 2003) agree in placing genus *Hedyosmum* as sister to the rest of
79 Chloranthaceae, and *Ascarina* as sister group to the clade *Chloranthus* + *Sarcandra*. Kong et
80 al. (2002) provided the first molecular phylogeny of *Chloranthus*, including all 10 recognized
81 species, while Zhang and Renner (2003) added 10 out of 20 *Ascarina* species and one of two
82 species of *Sarcandra* in their molecular phylogeny of Chloranthaceae. Attempts to solve
83 phylogenetic relationships within *Hedyosmum* have mainly been based on morphological
84 characters (Todzia, 1988; Eklund et al. 2004; see Appendix S2 for characteristic features).
85 However, the resulting cladograms suffered from low resolution or low support values,
86 probably due to a high degree of homoplasy. Zhang and Renner (2003) conducted the first
87 molecular phylogenetic study of all genera of Chloranthaceae, but were only able to include

1
2
3 88 five out of the 40-45 recognized species in *Hedyosmum* (Todzia 1988, 1993). Of particular
4
5 89 importance for understanding the biogeography of the genus is the position of the Asian
6
7 90 endemic *H. orientale*, whose phylogenetic position varied between studies: it was placed as
8
9 91 the sister of all *Hedyosmum* in Zhang and Renner (2003)'s molecular phylogeny but nested
10
11 92 among the Caribbean species in Eklund et al. (2004).

12
13 93 Based on a fossil-calibrated *rbcL*-ultrametric tree, Zhang and Renner (2003) estimated the
14
15 94 crown group diversification of *Hedyosmum* between 29 and 60 Ma (depending on calibration
16
17 95 point) and that of *Ascarina* and *Chloranthus* between 18–9 Ma and 22–11 Ma, respectively.
18
19 96 The remarkable “temporal gap” (~80 Ma) between the ancient age of the stem lineages of
20
21 97 Chloranthaceae and the late Cenozoic radiation of the extant species (crown groups) can also
22
23 98 be observed in the fossil record of *Hedyosmum*. Fossil pollen (“*Asteropollis*”) has been found
24
25 99 in numerous sites from the Early-Mid Cretaceous of Laurasia and Argentina, Africa, and
26
27 100 Australia, but after the Campanian in the Late Cretaceous no record has been recovered up to
28
29 101 the Early/Middle Miocene, when large amounts of pollen (“*Clavainaperturites*
30
31 102 *microclavatus*”) are reported from South America (Hoorn 1994; Wijninga 1996).

32
33 103 What has caused this large ‘temporal gap’? There are several possibilities. One is that the
34
35 104 ancestor lineage of *Hedyosmum* underwent a long period of little or low diversification,
36
37 105 followed by a recent, rapid radiation. Phylogenetic studies have pointed out the major role
38
39 106 played by the uplift of the tropical Andes in promoting rapid diversification of plant lineages,
40
41 107 either via ecological displacement (i.e., adaptive radiation) or through geographically induced
42
43 108 allopatric events (Hughes and Eastwood 2006; Moore and Donoghue 2007; Antonelli et al.
44
45 109 2009; see also Young et al., 2002 for a review). Most species of South American
46
47 110 *Hedyosmum* occur in montane habitats in the foothills of the Andes and the Central
48
49 111 Cordillera and it is thus possible that orogenic events associated with the Andean uplift
50
51 112 triggered diversification within this clade. If not the Andean uplift, Pleistocene climatic
52
53
54
55
56
57
58
59
60

1
2
3 113 changes could instead have fostered a rapid diversification in montane *Hedyosmum*, as has
4
5
6 114 been suggested for Neotropical birds (Weir 2006).

7
8 115 A second alternative is that the large temporal gap in Chloranthaceae is the result of
9
10 116 extinction events. High extinction rates, either punctual or constant, have a confounding
11
12 117 effect in the pattern of lineage accumulation of individual lineages. For example, Crisp and
13
14
15 118 Cook (2009) argued that a process of constant-rate diversification punctuated by a mass
16
17 119 extinction event produces a pattern of lineage diversification similar to the one expected from
18
19
20 120 a recent burst of speciation or adaptive radiation. Since the fossil record of Chloranthaceae
21
22 121 can be traced back to the Early Cretaceous, it seems likely that the family was affected by the
23
24 122 “impact winter” at the K/T event (65 Ma), when many woody magnoliid taxa went extinct
25
26
27 123 (Nichols 2007), or later by the Terminal Eocene event (35 Ma), when a dramatic cooling of
28
29 124 climates extirpated evergreen plant lineages that once formed part of the Holarctic
30
31
32 125 boreotropical flora (Tiffney 1985). Any of these extinction events could have extirpated the
33
34 126 old stem relatives that diverged prior to the extant crown radiation, leaving a reconstructed
35
36 127 phylogeny (i.e., a phylogeny that includes only extant taxa) with long stems and species-rich
37
38
39 128 crowns (Cook and Crisp 2009), a suitable description for Chloranthaceae (see Zhang and
40
41 129 Renner 2003: Fig. 2).

42
43 130 A third alternative is that the temporal gap observed between the stem and crown ages of
44
45
46 131 Chloranthaceae, especially in *Hedyosmum*, could be attributed to gradual high extinction
47
48 132 rates, possibly linked to the gradual cooling that followed the Early Eocene Climatic
49
50
51 133 Optimum (Zachos et al. 2001) and led to worldwide vegetational changes. Simulating
52
53 134 phylogenies with high background extinction rates – the ratio of extinction to speciation –
54
55 135 produces a pattern of lineage diversification resembling an increase in speciation rate through
56
57
58 136 time (Nee et al., 1994b). This effect, known as the “pull of the present”, occurs because
59
60 137 younger lineages are less likely to be removed by extinction than lineages that originated in

1
2
3 138 the past, so if extinction is high, nodes tend to concentrate near the tips (Pybus and Harvey
4
5 139 2000; Rabosky 2006b).

6
7
8 140 At last, the temporal gap could be an artifact of incomplete taxon sampling, which has
9
10 141 been shown to bias estimates of divergence times and diversification rates from reconstructed
11
12 142 phylogenies that do not include all extant species (Pybus and Harvey 2000; Linder et al.
13
14 143 2005; Cusimano and Renner 2010).

15
16
17 144 Here we use molecular dating, ancestral area reconstruction, and macro-evolutionary
18
19 145 birth-death models, to investigate the timing, tempo, and mode of diversification in
20
21 146 Chloranthaceae, with focus on the enigmatic genus *Hedyosmum*. In particular, we aim to
22
23 147 address the following questions: Does the diversification of Chloranthaceae and *Hedyosmum*
24
25 148 depart significantly from a constant rate model, and if so can this departure be explained by a
26
27 149 mass extinction event (e.g., K/T), gradual extinction, or by a recent rapid diversification? Did
28
29 150 the Asian endemic *H. orientale* originate by dispersal from the Neotropics, or is its currently
30
31 151 isolated distribution the result of vicariance of a once widespread Asian-American ancestor?
32
33 152 When did the Neotropical diversification of the genus occur? Could such diversification be
34
35 153 associated with the northern Andean uplift or with more recent events such as the closure of
36
37 154 the Panama Isthmus or Pleistocene climatic fluctuations?
38
39
40
41
42

43 155

44 156 MATERIALS AND METHODS

45 157 *Dataset*

46
47
48 158 A total of 40 species was included in the analysis, representing circa 62% of all
49
50 159 species in Chloranthaceae (see Online Table S1). These account for all species of
51
52 160 *Chloranthus* (10 sp.) and *Sarcandra* (2 sp.), and about half of all *Hedyosmum* (20 sp.) and
53
54 161 *Ascarina* species (10 sp.). The *Hedyosmum* species included here represent all subgenera,
55
56 162 sections, and informally recognized “species groups” in Todzia’s (1988) monograph, and
57
58
59
60

1
2
3 163 cover the total distribution of the genus. For the analyses that needed outgroup rooting,
4
5 164 *Ceratophyllum demersum* was chosen since it has been confidently shown to be closely
6
7
8 165 related to the Chloranthaceae but still not belong to it (see Endress and Doyle 2009 and
9
10 166 references therein for a discussion). All taxa included in this study are listed in the Online
11
12 167 Table S1, together with their GenBank accession numbers and voucher information.

15 168 Sequences for *Ascarina*, *Chloranthus*, and *Sarcandra* were obtained from GenBank.
16
17 169 Sequences for *Hedyosmum* were mostly obtained from field-collected leaf fragments dried
18
19 170 directly in silica gel. A few herbarium specimens did yield products after repeated trials, but
20
21 171 it is exceptionally difficult to amplify DNA from herbarium specimens of *Hedyosmum*
22
23 172 because the leaves contain ethereal oil cells and benzyloquinoline alkaloids (Dahlgren
24
25 173 1983) that probably affect DNA amplification. DNA was extracted and sequenced following
26
27 174 the protocols described in Antonelli (2008). In order to obtain phylogenetic resolution at
28
29 175 different levels of the ingroup, rather conservative markers were needed together with more
30
31 176 fast-evolving regions. After some pilot trials, a combination of markers was selected that
32
33 177 comprised the plastid *rbcL* gene and the *rps16* intron, and the nuclear ribosomal ITS region
34
35 178 (ITS 1 – 5.8S – ITS 2). Online Table S2 lists the primers used in this study.
36
37
38
39
40
41
42

43 180 *Alignment and Phylogenetic Analyses*

45 181 Sequences were aligned using the L-INS-I algorithm implemented in the software
46
47 182 MAFFT v. 6 (Kato et al. 2009). For the phylogenetic analyses, we used both maximum
48
49 183 parsimony (MP) and Bayesian inference (BI) methods as implemented in PAUP* 4.0b10
50
51 184 (Swofford 2002) and MrBayes 3.1.2 (Huelsenbeck and Ronquist 2001), respectively. For
52
53 185 parsimony analyses, a heuristic search was carried out using unweighted characters with 1000
54
55 186 replicates of random taxon addition sequence and 10 trees held at each step, and tree-
56
57
58 187 bisection-reconnection (TBR) branch swapping on best trees only, with a MaxTrees value of
59
60

1
2
3 188 100 and other standard settings. Bootstrap support values were estimated in PAUP* by
4
5
6 189 running 1000 replicates under Maximum Parsimony, using TBR branch swapping, and
7
8 190 saving multiple trees.

10 191 For the Bayesian phylogenetic analyses, we analyzed the dataset under three unlinked
11
12 192 partitions (ITS, *rbcL*, *rps16*). The best-fit model for each region was selected using the
13
14
15 193 Akaike Information Criterion (AIC) implemented in MrModelTest 2.2 (Nylander 2004). The
16
17 194 GTR+ Γ +I model of nucleotide substitution was chosen for ITS, while the HKY+ Γ +I and the
18
19
20 195 GTR+I models were selected as the best models for the plastid markers *rbcL* and *rps16*,
21
22 196 respectively. Bayesian analyses were initially run on each individual marker to compare them
23
24
25 197 for topology and node support. Since there was no significant incongruence between the
26
27 198 individual phylogenies, i.e., clades that were strongly supported (> 95% posterior probability
28
29 199 or 70% bootstrap value) in the 50% majority-rule consensus tree of one marker were also
30
31
32 200 present in the consensus trees of the other markers, we performed all subsequent analyses on
33
34 201 the concatenated dataset. Two simultaneous analyses with eight Metropolis-Coupled Markov
35
36 202 Chain Monte Carlo (MCMCMC) chains with incremental heating of 0.2 were run for 20
37
38 203 million generations and sampled every 1000 generations. Convergence of the MCMC was
39
40
41 204 assessed using the effective sampling size criterion for each parameter as implemented in
42
43
44 205 Tracer v. 1.4 (Rambaud and Drummond 2007) and the standard deviation of split frequencies
45
46 206 from MrBayes (Huelsenbeck and Ronquist 2001), and by monitoring cumulative posterior
47
48 207 probabilities and among-run variability of split frequencies using the online tool AWTY
49
50
51 208 (Nylander et al. 2008a). The first 4000 samplings (reflecting 400,000 generations) were
52
53 209 discarded as “burn in”, after checking for stability on the log-likelihood curves, and the
54
55 210 remaining trees from the independent runs (16,000 trees) were combined to build a 50%
56
57
58 211 majority rule consensus tree.

60 212

213 *Divergence Time Estimation*

214 To test if sequences evolved in a clocklike manner, we extracted the single Maximum
215 Likelihood (ML) tree out of 50 independent analyses using the software GARLI (Zwickl
216 2006) under a GTR+G+I model and other default settings. The tree was uploaded in PAUP
217 and likelihood scores computed with and without enforcing a molecular clock. A likelihood
218 ratio (LR) test was then performed in PAUP, with $LR = 2 (L_{\text{mol. clock enforced}} - L_{\text{no mol. clock}}$
219 $\text{enforced})$ and assumed to be distributed as a χ^2 with $S-2$ degrees of freedom, S being the
220 number of taxa in the dataset.

221 Since the LR test rejected the strict clock model ($p < 0.0001$), relative branching times
222 were estimated using two relaxed molecular clock approaches: the semi-parametric method
223 penalized likelihood (PL; Sanderson 2002) implemented in the program r8s version 1.70
224 (Sanderson 2003) and the Bayesian uncorrelated relaxed clock approach implemented in
225 BEAST v.1.4.8 (Drummond and Rambaut 2007). For the PL analysis, ultrametric branches
226 were calculated based on the topology of the 50% majority-rule consensus from the MCMC
227 Bayesian analysis, but with node ages estimated from mean branch lengths of 16,000 trees
228 from the Bayesian stationary sample. A cross-validation procedure was used to identify the
229 optimal smoothing value for the data, with \log_{10} increments of 0.1 and smoothing values
230 ranging from 0.1 to 7.9×10^5 , under the Truncated Newton algorithm and using the check
231 gradient function. To estimate age credibility values for nodes, 1000 trees randomly sampled
232 from the Bayesian posterior distribution of trees from the MCMC analysis were then
233 independently dated and the results summarized to obtain 95% confidence intervals of ages.
234 These values were calculated using the software TreeAnnotator (Drummond and Rambaut
235 2007) and visualized using FigTree v.1.1 (Rambaut 2008).

236 BEAST analyses were run on the Computational Biology Service Unit at Cornell
237 University, USA. Evolutionary models were coded separately for each sequence region, as

1
2
3 238 for the MrBayes analysis. Five independent runs of 10 million generations each using an
4
5 239 uncorrelated, lognormal, relaxed-clock model and a Yule prior on the tree were conducted.
6
7
8 240 Post burn-in trees were merged using LogCombiner (Drummond and Rambaut 2007) and
9
10 241 performance evaluated using Tracer. A maximum-clade credibility tree was computed and
11
12 242 95% confidence intervals of ages were calculated using TreeAnnotator. For the PL analysis,
13
14 243 *Ceratophyllum demersum* was pruned prior to the estimation of divergence times (since the
15
16 244 inclusion of an extra outgroup is required by the program). For the BEAST analysis, we only
17
18 245 included Chloranthaceae taxa.
19
20
21

22 246 To obtain absolute divergence times, we used the rich fossil record of Chloranthaceae
23
24 247 (Eklund et al. 2004). The oldest undisputable fossils of the family are *Hedyosmum*-like
25
26 248 female flowers from the Late Aptian or Early Albian of Portugal associated with pollen of
27
28 249 *Asteropollis* (Friis et al. 1994, 1997). Although these fossils were originally described as
29
30 250 being from the Barremian-Aptian, newer evidence indicates that the sediments in which they
31
32 251 were found are rather Late Aptian – Early Albian (Hochuli et al. 2006). These fossils were
33
34 252 inferred to represent a stem relative of *Hedyosmum* (Eklund et al. 2004) and thus provide a
35
36 253 minimal age for the Chloranthaceae at 110 Ma. This age was used to constrain the age of the
37
38 254 root node in the phylogeny: as a fixed age in the PL analysis, and as a prior with a lognormal
39
40 255 distribution (offset = 110, standard deviation = 0.5) in the BEAST analysis. Other fossils
41
42 256 include *Chloranthus*-like stamens from the Late Cretaceous of New Jersey (USA) and
43
44 257 Sweden (*Chloranthistemon crossmanensis*; Herendeen et al. 1993). These fossils were
45
46 258 inferred to be sister to all extant species of *Chloranthus* (Eklund et al. 2004) and thus provide
47
48 259 a minimal stem age for the genus at 92 Ma (coded as a lognormal prior in BEAST, with
49
50 260 standard deviation of 1.0). These two sets of fossils are the same calibration points used by
51
52 261 Zhang and Renner (2003) for obtaining absolute ages from an ultrametric tree inferred from
53
54 262 the *rbcL* gene. However, in their study two independent datings were performed, which
55
56
57
58
59
60

1
2
3 263 resulted in ages that generally differed by a factor of two. Since we considered these two sets
4
5 264 of fossils equally reliable in terms of identification, taxonomic placement, and geologic age,
6
7
8 265 and since multiple calibration points have been suggested to increase precision in divergence
9
10 266 time estimates (Britton 2005), here we used both of them simultaneously to calibrate different
11
12 267 nodes of the trees.
13
14

15 268
16
17 269 *Biogeographic Analyses*

18
19
20 270 Operational areas for biogeographic analyses were defined as geographic ranges shared by
21
22 271 two or more species and delimited by geological features that may have acted as barriers to
23
24 272 dispersal (Sanmartín 2003). In order to maximize congruence with other biogeographic
25
26 273 studies in the region, we used here the same operational areas as in Antonelli et al. (2009)
27
28 274 (see Fig. 3a inset for area delimitation): (A) *Central America*, (B) *West Indies*, (C) *Northern*
29
30 275 *Andes* (10° N – 5° S), (D) *Central Andes* (5° S – 18° S), (E) *Chocó region*, (F) *Guiana Shield*,
31
32 276 (G) *Southeastern South America*, and (H) *Australasia*. Distribution data for species were
33
34 277 compiled from Todzia (1988), GBIF (www.gbif.org), and herbarium specimens.
35
36
37

38 278 To infer the ancestral areas and biogeographic history of Chloranthaceae, we used two
39
40 279 character state reconstruction methods: Fitch Optimization, implemented in the software
41
42 280 MESQUITE v. 2.0.1 (Maddison and Maddison 2007), and Dispersal-Vicariance Analysis
43
44 281 (Ronquist 1997), implemented in the program DIVA v. 2.1 (Ronquist 2001). Fitch
45
46 282 Optimization constrains ancestors to be restricted to single areas and models range evolution
47
48 283 as a change in character state from ancestor to descendant, equivalent to dispersal between
49
50 284 single areas. DIVA, in contrast, allows widespread distributions at ancestral nodes, which are
51
52 285 divided at speciation events by vicariance, and models dispersal as range evolution along the
53
54 286 internodes leading to the (vicariant) speciation event, i.e., dispersal leads to vicariance but it
55
56 287 is not directly associated with speciation (Sanmartín 2007). Therefore, the two methods can
57
58
59
60

1
2
3 288 be said to implement alternative biogeographic evolutionary models: a dispersalist (Fitch) vs.
4
5 289 vicariancist (DIVA) approach. DIVA analyses were run unconstrained (all possible areas
6
7
8 290 allowed). To account for phylogenetic uncertainty in the parsimony biogeographic
9
10 291 reconstruction, we used the Bayes-DIVA approach (Nylander et al. 2008b) and Mesquite
11
12 292 (Maddison and Maddison 2007) to infer ancestral area distributions and biogeographic events
13
14
15 293 in 1000 trees randomly sampled from the stationary distribution of the Bayesian MCMC
16
17 294 analysis. We then computed the relative frequencies of ancestral area reconstructions across
18
19
20 295 the 1000 trees for each node in the 50% majority-rule Bayesian consensus tree. For Fitch
21
22 296 Parsimony, widespread taxa were coded as equivocal, since Mesquite does not allow multiple
23
24
25 297 area coding.

26
27 298 Parsimony-based biogeographic methods such as Fitch Optimization or DIVA optimize
28
29 299 ancestral areas onto the nodes of a phylogeny by minimizing the number of events, dispersal
30
31 300 and extinction, that lead to a change in the geographic range of a taxon. In contrast,
32
33
34 301 parametric methods such as Dispersal-Extinction-Cladogenesis (DEC, Ree et al. 2005) -
35
36 302 implemented in the software LAGRANGE v. 2.0 (Ree and Smith 2008) - are based on a
37
38
39 303 stochastic model of biogeographic evolution that specifies the rate of transition between
40
41 304 geographic ranges along phylogenetic branches as a function of time, thus overcoming the
42
43
44 305 parsimony bias of underestimating the number of changes along branches (Ree & Sanmartin
45
46 306 2009). Given a time-calibrated phylogeny, the distribution of terminal species, and a
47
48
49 307 transition probability matrix specifying the rate of change between geographic ranges as
50
51 308 dispersal (range expansion) and extinction (range contraction) parameters, LAGRANGE
52
53 309 allows estimating the dispersal and extinction rates and the probabilities of range inheritance
54
55
56 310 scenarios using maximum likelihood inference algorithms (Ree and Smith 2008). One
57
58 311 limitation of the DEC approach – and parametric methods in general – is that the number of
59
60 312 biogeographic parameters to estimate from the data increases exponentially with the number

1
2
3 313 of areas, increasing computational time and decreasing the inferential power of the model
4
5 314 (Ree and Sanmartín 2009). Since most species of *Hedyosmum* are confined to one or two
6
7
8 315 operational areas, we constrained widespread states in our model to include only ancestral
9
10 316 ranges that span a maximum of two areas. Thus, our LAGRANGE analysis can be said to
11
12 317 provide an intermediate approach between the Fitch (“single-area”) analysis and the
13
14 318 unconstrained (“all-areas”) DIVA analysis. LAGRANGE requires a fully bifurcated tree, so
15
16 319 we used the “allcompat” consensus phylogram from MrBayes (50% majority rule consensus
17
18 320 with all compatible groups added) with branch lengths equaling mean node ages estimated by
19
20 321 PL.
21
22
23
24
25
26

27 323 *Diversification Tests*

28
29 324 To test whether the temporal pattern of lineage diversification in Chloranthaceae departs
30
31 325 from a constant-rate model, we used the gamma statistic (Pybus and Harvey 2000)
32
33 326 implemented in the R package LASER v. 2.1. (Rabosky 2006a). The gamma statistic is a
34
35 327 measurement of the node spread across a phylogeny that compares the relative position of
36
37 328 node ages in a phylogenetic tree to that expected under a pure birth (Yule) model in which
38
39 329 the speciation rate is constant over time (Yule 1924). Values lower than 0 ($\gamma < 0$) or higher
40
41 330 than 0 ($\gamma > 0$) indicate, respectively, that internode distances are longer or shorter towards the
42
43 331 recent than expected under the Yule model (Pybus and Harvey 2000). Incomplete taxon
44
45 332 sampling has a non-random effect on the distribution of branch lengths in a phylogenetic tree
46
47 333 and can therefore bias temporal-based diversification tests (Pybus and Harvey 2000). For the
48
49 334 gamma test, incomplete taxon sampling would result in an apparent decrease of speciation
50
51 335 rates towards the present, lowering the value of the gamma statistic and leading to incorrectly
52
53 336 rejecting the null hypothesis of constant-rate diversification (Rabosky 2006b). Our phylogeny
54
55 337 of Chloranthaceae covers only 62% of the extant diversity in the family (40 species out of
56
57
58
59
60

1
2
3 338 65), so we used the Monte Carlo constant rates (MCCR) test developed by Pybus and Harvey
4
5 339 (2000) to correct the gamma statistic value. We simulated 5000 phylogenetic trees with 65
6
7 340 taxa under the Yule model (using the estimated pure speciation value, see below), and
8
9 341 randomly sampled 40 taxa from each tree to obtain a phylogeny with the same number and
10
11 342 size as the empirical phylogeny. We then computed the gamma statistics for each of the
12
13 343 simulated phylogenies and compared the observed empirical gamma value against the
14
15 344 distribution of gamma values from the simulated phylogenies using the *mccrTest* in LASER.

16
17
18
19 345 Second, we used birth-death likelihood (BDL) tests implemented in LASER to detect
20
21 346 temporal shifts in diversification rates in the phylogeny of Chloranthaceae. The ΔAIC_{RC}
22
23 347 test (Rabosky 2006b) was used to statistically evaluate the fit of the temporal pattern of
24
25 348 lineage diversification in Chloranthaceae to a set of rate-constant and rate variable models: i)
26
27 349 a pure birth (Yule) model; ii) a constant-rate birth-death model in which there is a speciation
28
29 350 rate (b) and an extinction rate (d) parameter and the net diversification rate ($b - d$) is constant
30
31 351 through time (Nee et al., 1992; 1994a,b); and iii) a rate-variable Yule model in which there is
32
33 352 one (Yule-2-rate) or two (Yule-3-rate) shifts in the speciation rate (Rabosky 2006a,b). We
34
35 353 estimated the difference in AIC score between the best rate-constant model and the best rate
36
37 354 variable model for the original chronogram ($\Delta AIC_{RC} = AIC_{RC} - AIC_{RV}$), and then compared
38
39 355 this value to a distribution of ΔAIC_{RC} scores for 100 phylogenies simulated under a rate-
40
41 356 constant Yule model using the original number of taxa and the ML birth rate estimated by
42
43 357 LASER.

44
45
46
47
48
49
50
51 358 The *allcompat* consensus from MrBayes with branch lengths reflecting mean nodal ages
52
53 359 obtained with PL and excluding the outgroup *Ceratophyllum demersum*, was used as the
54
55 360 empirical chronogram of Chloranthaceae for the gamma and ML birth-death tests.
56
57 361 Alternatively, we used the BEAST chronogram, but both methods gave very similar results
58
59 362 since age estimates were also very similar (see below). We repeated these analyses for the
60

Antonelli and Sanmartín, *Spatiotemporal evolution of Hedyosmum* Page 16 (51)

1
2
3 363 *Hedyosmum* stem clade and the *Hedyosmum* crown group, using the PL ingroup chronogram
4
5 364 of Chloranthaceae pruned to include the split between *Hedyosmum* and *Chloranthus spicatus*
6
7
8 365 as the root node of the *Hedyosmum* stem clade. The first split within genus *Hedyosmum*,
9
10 366 separating a Caribbean clade from the *Hedyosmum orientale-Tafalla* group, was used as the
11
12
13 367 root node of the *Hedyosmum* crown group (see Fig. 3).

14
15 368 BDL tests in LASER assume complete taxon sampling of the extant phylogeny and this
16
17 369 may bias the estimation of parameter values and the testing of diversification models.
18
19 370 Rabosky et al. (2007) described a method that combines phylogenetic and taxonomic
20
21 371 (species-richness) data to account for incomplete taxon sampling while testing for
22
23 372 diversification rate shifts across branches in a phylogeny. Alfaro et al. (2009) extended this
24
25 373 method to a stepwise AIC approach, “MEDUSA”, implemented in the R package GEIGER
26
27 374 (Harmon et al. 2003), which allows testing for multiple shifts in diversification rates on an
28
29 375 incompletely resolved phylogeny. The PL ingroup chronogram of Chloranthaceae was
30
31 376 pruned to include each major lineage within the family. This chronogram and information on
32
33 377 the total number of species within each lineage was used to compare the net rate of
34
35 378 diversification over the entire phylogeny of Chloranthaceae with a model in which there is
36
37 379 one or multiple shifts in diversification rate along branches in the phylogeny. Genera
38
39 380 *Ascarina* (20 species) and *Sarcandra* (2 spp.) were represented by one lineage each, while
40
41 381 *Chloranthus*, for which taxon sampling was complete (10 species), was divided into two
42
43 382 major clades: “nervosus” and “spicatus” (5 species each, Kong et al. 2002). *Hedyosmum* was
44
45 383 divided into three main lineages (*H. nutans*, representing the Central-American clade (3
46
47 384 species), *H. orientale* (1 species), and *H. arborescens* representing the South American
48
49 385 subgenus *Tafalla* (40 species).
50
51
52
53
54
55
56

57 386

58
59 387 *Comparing Empirical versus Simulated Phylogenies*
60

1
2
3 388 Comparing the shape of lineage-through-time (LTT) plots of empirical phylogenies
4
5
6 389 against those of phylogenies simulated under alternative diversification models can help to
7
8 390 understand the effect of macro-evolutionary processes, such as speciation and extinction, on
9
10 391 the temporal pattern of lineage diversification of individual lineages (Harvey et al. 1994;
11
12 392 Cook and Crisp 2009). One advantage of simulations is that the effect of incomplete taxon
13
14
15 393 sampling may be incorporated to the age structure of the simulated phylogenies – and
16
17 394 corresponding LTT plots – by simulating phylogenies conditional on the current extant
18
19 395 diversity (e.g., 65 species in Chloranthaceae), and then randomly sampling species from the
20
21 396 reconstructed phylogenies to reflect the size and sample of the empirical phylogeny (40
22
23 397 species). These simulations can then be used to visually explore the departure of the
24
25 398 empirical LTT plot from constant-rate and episodic birth death models while incorporating
26
27 399 the effect of incomplete taxon sampling.
28
29
30

31
32 400 We used the R package APE (Paradis et al. 2004) to generate the lineage-through-
33
34 401 time (LTT) plot of Chloranthaceae from the PL ingroup chronogram and overlaid this onto
35
36 402 the LTT plots of 100 phylogenies simulated under a 2:1 birth-death model, using the birth
37
38 403 rate estimated by LASER under the “purebirth” model ($b=0.046$; Table 2) and accounting for
39
40 404 incomplete taxon sampling as described above. Simulated phylogenies were rescaled with the
41
42 405 APE function *chronoPL* using the Barremian-Aptian fossil (110 Ma) to calibrate the root
43
44 406 node. We repeated this procedure for the *Hedyosmum* stem clade and the *Hedyosmum* crown
45
46 407 group, simulating the phylogenies to 44 extant species (24 sampled) for the *Hedyosmum* stem
47
48 408 clade and 43 species (23 sampled) for the *Hedyosmum* crown group in order to account for
49
50 409 incomplete taxon sampling. We used the split between *Chloranthus* and *Hedyosmum* in the
51
52 410 PL chronogram to date the root node of the *Hedyosmum* stem lineage (110 Ma, see Fig. 3),
53
54 411 and the first split between the Caribbean clade and the *H. orientale-Tafalla* group as the age
55
56 412 of the root node of the *Hedyosmum* crown group (36 Ma).
57
58
59
60

1
2
3 413 We also used simulations to visually explore the effect of alternative extinction
4
5 414 scenarios on the pattern of lineage accumulation through time in Chloranthaceae. First, we
6
7 415 examined whether an episodic birth death model – a process of constant-rate diversification
8
9 416 punctuated by a mass extinction event (Cook & Crisp, 2009) – could produce a temporal gap
10
11 417 between stem and crown ages similar to the one observed in Chloranthaceae. We simulated
12
13 418 phylogenies in which two episodes of constant birth-death growth are interspersed with an
14
15 419 episode of mass extinction that eliminates a large percentage of extant lineages. Simulations
16
17 420 were conditioned on reaching 65 extant species and on the mass extinction event happening
18
19 421 at a fixed time before the present, either 65 Ma (the K/T event) or 35 Ma (the Terminal
20
21 422 Eocene cooling event). To account for incomplete taxon sampling, we sampled a fraction of
22
23 423 the extant species at the end of the second birth-death growth episode (probability of
24
25 424 sampling an extant species = $40/65 = 0.62$).

26
27
28
29
30
31 425 A critical point in our simulations is to decide the severity of the mass extinction
32
33 426 event – the percentage of lineages that go extinct – and the birth/death values adopted by the
34
35 427 constant-rate diversification model before and after the mass extinction. We used a “visual”
36
37 428 approach to parameter tuning, in which we started with the ML values of speciation and
38
39 429 extinction estimated by LASER and gradually changed the background extinction rate of the
40
41 430 birth death process ($a = d/b$ from 0.5 to 0.95), and the intensity of the punctual mass
42
43 431 extinction event or probability of lineage survival (from 0.50% to 0.05%) in an attempt to
44
45 432 obtain phylogenies with the anti-sigmoid shape of the Chloranthaceae LTT plot, a similar
46
47 433 root age (100 Ma), and a large temporal gap between stem and crown ages. We explored
48
49 434 models in which the speciation and extinction rates were the same before and after the mass
50
51 435 extinction, as well as models in which they differed between the first and second growth
52
53 436 phases (“fast growth–mass extinction–slow growth”, “slow growth–mass extinction–fast
54
55 437 growth”) as in Cook and Crisp (2009). One hundred phylogenies were generated per model to

1
2
3 438 reflect the stochastic variance. Admittedly, our visual approach to parameter tuning is not
4
5
6 439 optimal but we lack a maximum likelihood function for the episodic birth-death model, as it
7
8 440 is available for the constant-rate birth death model (see Stadler 2011). Moreover, our aim
9
10 441 here was not to estimate the parameters from the data but to answer the question: Can a group
11
12 442 this old (120-110 Ma) and with such low extant diversity (65 species) be explained by a mass
13
14
15 443 extinction model, and does the shape of the LTT plots simulated under this model resemble
16
17 444 that of our empirical chronogram?

19
20 445 Constant high relative extinction rates can also produce a pattern of lineage
21
22 446 accumulation that resembles a sudden acceleration of diversification rates through time (Nee
23
24 447 et al., 1994b; Rabosky 2006b; Rabosky and Lovette 2008). To explore this possibility, we
25
26
27 448 simulated phylogenies under a constant-rate birth death model using the ML values estimated
28
29 449 by LASER ($b = 0.082$, $d = 0.067$; $a = 0.78$, Table 2), and compared these with phylogenies
30
31
32 450 simulated under a birth death model with high background extinction ($a = d/b = 0.95$), using
33
34 451 the ML speciation rate estimated by LASER under the Yule model. We then compared the
35
36 452 shape of the resulting phylogenies and corresponding LTT plots against those of the
37
38
39 453 Chloranthaceae chronogram and the mass extinction models.

40
41 454 Several studies have used a similar approach to ours – comparing empirical and
42
43 455 simulated phylogenies under alternative birth-death models – to understand the effect of
44
45
46 456 macro-evolutionary processes on patterns of lineage diversification. Proper comparison
47
48 457 requires the simulations to be drawn from the right null tree distribution. Most of these
49
50
51 458 studies have used PHYLOGEN v.1.1 (Rambaut 2002) as tree sampler to simulate phylogenies
52
53 459 under rate-constant (Weir 2006) or rate-variable (Crisp and Cook 2009) models. Hartmann et
54
55 460 al. (2010), however, demonstrated that when conditioning on the number of species (n),
56
57
58 461 PHYLOGEN generates unrealistic null tree distributions and may produce trees with incorrect
59
60 462 branch lengths and/or shapes. Specifically, simulations in PHYLOGEN are stopped after the

1
2
3 463 tree first reaches n species, so the species produced by the last speciation event have zero
4
5 464 branch lengths and later periods with n species are disregarded. This has the effect that
6
7
8 465 simulated trees in PHYLOGEN are consistently younger than expected (Hartman et al. 2010).
9
10 466 To avoid this, in our study we simulated phylogenies under the general sampling model
11
12 467 described by Hartman et al. (2010) and implemented in the program TreeSim (Stadler 2011),
13
14 468 which correctly simulates trees conditional of n species using a point process approach that
15
16 469 also incorporates incomplete sampling (Stadler 2008, 2009, 2011). This is done by
17
18 470 stochastically sampling taxa from the reconstructed phylogeny, which has been generated
19
20 471 conditioning on the extant diversity. For the episodic birth-death process, and unlike
21
22 472 PHYLOGEN (Cook and Crisp 2009), TreeSim simulates trees properly by going backward in
23
24 473 time conditioning on both n final extant species and the mass extinction event occurring at a
25
26 474 specific fixed time *before* the present (Stadler 2011). We also used TreeSim simulations to
27
28 475 generate the null distribution of Yule phylogenies for the deltaAICRC and gamma tests –
29
30 476 rather than using LASER's own simulation tools – to avoid problems with incorrect null
31
32 477 distributions. The effect of incomplete taxon sampling in the age distribution of the simulated
33
34 478 phylogenies was accounted for by simulating to extant diversity and randomly sampling taxa
35
36 479 from the reconstructed tree as described above. All R and TreeSim scripts used here can be
37
38 480 obtained from I.S. on request.
39
40
41
42
43
44
45
46
47
48
49
50
51
52
53
54
55
56
57
58
59
60

482 RESULTS

483 *Phylogeny*

484 The aligned data matrix comprised 2771 characters, of which 1398 were derived from
485 *rbcL*, 697 from *rps16*, and 676 from ITS. Out of 558 variable characters, 352 were parsimony
486 informative. Figure 1 and Appendix S3 show the cladogram and the phylogram, respectively,
487 of the 50% majority-rule consensus tree of the Bayesian stationary sample ($n = 16000$ trees).

1
2
3 488 The consensus tree from the parsimony analysis was congruent with the Bayesian consensus,
4
5 489 in the sense that there were no clades that were strongly supported (> 70% bootstrap support,
6
7
8 490 > 95% posterior probability) in one tree but contradicted in the other. The trees and dataset
9
10 491 produced in this study are available from <http://www.treebase.org>, study number 11151.

11
12 492 Relationships among genera were consistent with previous studies (Zhang and Renner
13
14 493 2003; Eklund et al. 2004). The Old World genera *Ascarina*, *Sarcandra*, and *Chloranthus*
15
16 494 form together a strongly supported clade, sister to *Hedyosmum* (1.00 BPP, 100% BS; Fig. 1).
17
18 495 *Sarcandra* and *Chloranthus* are together sister to *Ascarina* (0.98 BPP, 93% BS). Similarly,
19
20 496 infrageneric relationships that are strongly supported in *Ascarina*, *Sarcandra*, and
21
22 497 *Chloranthus* are all corroborative of the results of previous works (Zhang and Renner 2003;
23
24 498 Eklund et al. 2004).

25
26 499 Inter-specific resolution was high within *Hedyosmum*, with over 90% of all internal nodes
30
31 500 appearing in the 50% majority-rule tree from the Bayesian analysis (Fig. 1). The first split in
32
33 501 the genus separates a clade comprising the Antillean species *H. nutans*, *H. grisebachii*, and
34
35 502 *H. domingense* from all other species. These three species are small (up to 1.5 m tall) shrubs
36
37 503 endemic to Cuba and Hispaniola (*H. grisebachii* is only known from Cuba). The close
38
39 504 relationship between *H. nutans* and *H. grisebachii* corroborates the results by Eklund et al.
40
41 505 (2004) based on morphological data, although their study did not include *H. domingense*. The
42
43 506 sister group to the Antillean taxa is a clade comprising *Hedyosmum orientale* sister to all the
44
45 507 remaining species. *Hedyosmum orientale* is the type species of subgenus *Hedyosmum*
46
47 508 (Todzia 1988). Since *H. nutans*, *H. grisebachii*, and *H. domingense* were also placed in this
48
49 509 group, subgenus *Hedyosmum* is shown here to be paraphyletic. Within this subgenus, section
50
51 510 *Orientalis* comprised *H. grisebachii*, *H. domingense*, and *H. orientale*. Our results also
52
53 511 indicate that section *Orientalis* is paraphyletic as currently circumscribed.
54
55
56
57
58
59
60

1
2
3 512 All the remaining species of *Hedyosmum* sequenced belong with strong support to
4
5 513 subgenus *Tafalla* (Fig. 1), corroborating earlier studies (Todzia 1988; Zhang and Renner
6
7 514 2003; Eklund et al. 2004). However, within subgenus *Tafalla*, the three sections proposed
8
9 515 (*Microcarpa*, *Macrocarpa*, and *Artocarpoides*) fail to reflect phylogenetic relationships by
10
11 516 either being paraphyletic (*Microcarpa* and *Macrocarpa*) or monotypic (*Artocarpoides*, Fig.
12
13 517 1).
14
15
16
17
18
19

20 519 *Age Estimates and Ancestral Range Reconstruction*

21
22 520 Figure 2 and Appendices S4–S7 show the chronograms obtained by the PL and BEAST
23
24 521 analyses. Age estimates from PL and BEAST were fairly similar, with considerable overlap
25
26 522 in the 95% confidence intervals / highest posterior densities (Table 1). Moreover, our age
27
28 523 estimates for the family and the four genera under the two dating analyses generally agreed
29
30 524 with those obtained by Zhang and Renner (2003) using their preferred fossil calibration
31
32 525 (Table 1).
33
34
35

36 526 Figures 3 and 4 show the results from ancestral area reconstructions obtained with Fitch
37
38 527 Parsimony/Bayes-DIVA and LAGRANGE, respectively, plotted on the PL mean age
39
40 528 chronogram of Chloranthaceae. In general, reconstructions are ambiguous about the origin of
41
42 529 Chloranthaceae and differ among methods. The unconstrained Bayes-DIVA analysis (Fig.
43
44 530 3b) supports an ancestor that was widely distributed in the Old and New World (ABCDH),
45
46 531 including all the regions where it is present today except for some regions in South America,
47
48 532 the Chocó (E), Guiana (F), and southeastern South America (G). LAGRANGE (Fig. 4)
49
50 533 indicates an American-Australasian (HB) or an Australasian origin (H) with almost equal
51
52 534 relative probability, whereas Fitch reconstructions are ambiguous, with no clear origin
53
54 535 supported (Fig. 3a). For *Hedyosmum*, Fitch Parsimony is also ambiguous but shows higher
55
56 536 support for an Australasian or American origin (slightly higher for Australasia, Fig. 3a),
57
58
59
60

1
2
3 537 whereas Bayes-DIVA infers a widespread Old-New World origin, including the Neotropics
4
5 538 (ABCDH, Fig. 3b). LAGRANGE also supports an Australasian-American origin for
6
7
8 539 *Hedyosmum* but excluding the Neotropics (HB, Fig. 4). Both Fitch Parsimony and
9
10 540 LAGRANGE infer colonization of South America sometime during the Early-Middle
11
12 541 Miocene (17-15 Ma), apparently using the northern Andes (area C) as a dispersal route
13
14
15 542 southwards (Figs. 3a, 4). From the Northern Andes, dispersal back to Central America (area
16
17 543 A) occurred at least three times: one leading to *H. mexicanum*, possibly before the final
18
19 544 closure (uplift) of the Panama Isthmus ~3.5 Ma (as indicated by Bayes-DIVA; Fig. 3b); and
20
21
22 545 two others after its closure, one leading to *H. scaberrimum*, and the other to *H. goudotianum*
23
24 546 with its sister taxa *H. correanum* and *H. bonplandianum* (Figs. 3, 4). Dispersal to
25
26 547 southeastern Brazil (area G) in *H. brasiliense* and the Guiana Shield (area F) in *H.*
27
28 548 *racemosum* occurred relatively recently, apparently in the Late Miocene-Pliocene (Figs. 3, 4).
29
30
31
32
33

34 550 *Diversification models*

35
36 551 The gamma test rejected a constant-rate diversification model, even after correcting
37
38 552 for incomplete taxon sampling, for both Chloranthaceae (2.241, $p > 0.999$) and the
39
40 553 *Hedyosmum* stem clade (2.554, $p > 0.999$; Table 2). In contrast, the gamma test did not reject
41
42 554 rate constancy for the *Hedyosmum* crown group (- 0.382, $p = 0.7426$; Table 2). Although
43
44 555 strictly the gamma test can only be used for testing a model of decreasing speciation rates
45
46 556 through time against a constant-rate diversification model (Pybus and Harvey 2000), highly
47
48 557 positive values of the gamma statistic are generally interpreted as indicating an increase of
49
50 558 speciation rates through time (Weir 2006). A comparison of the observed gamma value for
51
52 559 Chloranthaceae against the distribution of values from the 5000 simulated incomplete
53
54 560 phylogenies shows that the observed value falls outside the 99% right tail confidence interval
55
56 561 (critical value at 5% level = -2.014).
57
58
59
60

1
2
3 562 The gamma statistic is a powerful tool to test if a constant rate speciation model is
4
5
6 563 plausible for a given phylogeny. Birth-death likelihood (BDL) methods, on the other hand,
7
8 564 incorporate extinction and can be used to explicitly test the fit of a constant-rate birth-death
9
10 565 model (a constant-rate model with $d > 0$) against a time-varying speciation model (Rabosky,
11
12 566 2006b). The ΔAIC_{RC} test in LASER indicated a significant departure of the lineage
13
14
15 567 cumulative curve of Chloranthaceae from a model of constant-rate diversification ($\Delta AIC_{RC} =$
16
17 568 7.689, $p < 0.001$, Table 2). The model with the lowest AIC score was a Yule-3-rate variable
18
19 569 model with two shifts in diversification rate: an increase at 23 Ma and a rate decrease at 2.1
20
21
22 570 Ma (Table 2). The first shift is particularly abrupt, with an eight-fold increase in the rate of
23
24 571 diversification in comparison with the previous rate: $r_1 = 0.015$, $r_2 = 0.080$. It corresponds to
25
26 572 the branching point between *Hedyosmum orientale* and subgenus *Tafalla* (Fig. 3, red arrow).
27
28
29 573 The best-fit constant-rate model was a birth-death model with a high relative extinction rate
30
31 574 (extinction ratio $a = b/d = 0.82$, Table 2). For the *Hedyosmum* stem clade, the best-fitting
32
33 575 model was also a Yule-3-rate variable model with an increase in diversification rate at 23 Ma
34
35 576 and a decrease at 3.5 Ma (Table 2). However, this model is only marginally significantly
36
37 577 better ($\Delta AIC_{RC} = 1.587$, $p = 0.049$) than a constant-rate model with a very high extinction
38
39 578 fraction ($a > 0.999$). In contrast, the ΔAIC_{RC} test rejected a temporal shift in
40
41
42 579 diversification rates for the *Hedyosmum* crown group ($\Delta AIC_{RC} = 0.868$, $p = 0.099$; Table 2).
43
44 580 The model with the lowest AIC was a Yule-2-rate model with a rate decrease at 3.5 Ma, but
45
46 581 there was no significant difference with a pure-birth model with speciation rate $r = 0.080$
47
48 582 (Table 2). The ML estimate of the extinction fraction for the *Hedyosmum* crown group was
49
50 583 very low ($a = 0$; 95% confidence interval: 0-0.4).

51
52
53 584 Unlike BDL methods, the MEDUSA combined phylogenetic-taxonomic approach allows
54
55 585 the rate of diversification to vary among lineages - although it assumes rate constancy
56
57 586 through time within each major lineage (Rabosky et al. 2007). MEDUSA detected one

1
2
3 587 significant shift in diversification rates in the branch leading to the *H. arborescens* lineage,
4
5 588 which represents subgenus *Tafalla*. Specifically, there was a ten-fold increase in the rate of
6
7
8 589 diversification between this clade, grouping all South American species of *Hedyosmum* ($r_2 =$
9
10 590 0.125 ; $b = 0.286$, $d = 0.161$; $a = 0.562$), and the remainder of the tree ($r_1 = 0.014$; $b = 0.052$, d
11
12 591 $= 0.041$; $a = 0.78$).

15 592 The LTT plot of the empirical chronogram of Chloranthaceae shows an initial period of
16
17 593 diversification (110-90 Ma), followed by a phase of little or no diversification between 90
18
19 594 and 40 Ma (the long stem or ‘temporal gap’), and a final upturn in the rate of diversification
20
21
22 595 at around 20 Ma (Fig. 5a). A similar pattern can be observed in the LTT plot of the
23
24 596 *Hedyosmum* stem lineage, with a long stem and a late upturn in the pattern of lineage
25
26
27 597 accumulation at 23 Ma (Fig. 5b). In contrast, the LTT plot of the *Hedyosmum* crown group
28
29 598 shows a more exponential pattern of lineage accumulation, characteristic of a constant birth-
30
31
32 599 death rate process with a low extinction rate (Fig. 5c). Comparison with simulated
33
34 600 phylogenies under a 2:1 birth-death diversification model – pruned to reflect incomplete
35
36 601 taxon sampling – shows that the empirical LTT plot falls outside the 95% confidence interval
37
38 602 generated by the simulations in Chloranthaceae and the *Hedyosmum* stem lineage (Fig. 5a,b),
39
40
41 603 but falls marginally within in the *Hedyosmum* crown group (Fig. 5c).

43 604 Appendix S8 shows the LTT plots of simulation attempts for the episodic 65 Ma birth
44
45 605 death model. Many simulations resulted in trees far too young compared to the empirical
46
47 606 chronogram, especially for the 65 Ma model (Appendix S8). The best combination of
48
49 607 parameter values for the two mass extinction scenarios (65 and 35 Ma) – resulting in
50
51
52 608 phylogenies with 65 extant species and a basal divergence close to the root age of
53
54 609 Chloranthaceae (120-100 Ma) – was achieved with a first episode of birth-death growth (e.g.,
55
56 610 $a = d/b = 0.5$), followed by a severe mass extinction event that extirpated 95% percent of
57
58
59 611 extant lineages, and ending in a second episode with slow growth and a high background

1
2
3 612 extinction ($a = b/d = 0.95$, Fig. 6a,b). The reconstructed phylogenies all exhibit the expected
4
5 613 “broom and handle” shape (Crisp & Cook, 2009), with long stems and species-rich crowns,
6
7 614 and large temporal gaps between stem and crown ages (90-50 million years, see Appendix
8
9 615 S9-S10). The LTT plots show the classic anti-sigmoid pattern (Harvey et al. 1994), with an
10
11 616 initial period of diversification, followed by a plateau (the “stem”), and a final upturn in the
12
13 617 pattern of lineage accumulation (Fig. 6a,b), similar to the one exhibited by the empirical
14
15 618 phylogeny of Chloranthaceae (Fig. 5a). In LTT plots of mass extinction models, the mass
16
17 619 extinction event precedes the end of the plateau (Harvey et al. 1994; Cook and Crisp 2009).
18
19 620 In the empirical LTT plot of Chloranthaceae, the end of the plateau falls around 36 Ma,
20
21 621 showing a better fit to the 35 mass extinction model than to the 65 Ma model. However, in
22
23 622 our simulations, especially for the 65 Ma model, there was not always a close correspondence
24
25 623 between the time of the mass extinction event – as observed in the complete phylogeny
26
27 624 including extinct species (Appendix S9) - and the upturn in the rate of diversification in the
28
29 625 LTT plot of the corresponding reconstructed (incompletely sampled) phylogeny. In some
30
31 626 curves, the start of diversification seemed to be delayed, perhaps an effect of incomplete
32
33 627 taxon sampling randomly removing lineages that started diversifying right after the mass
34
35 628 extinction event.

36
37 629 The LTT plots of the constant high relative extinction models (Fig. 6c,d) generally
38
39 630 showed a shorter plateau and a less steeper pattern than the LTT plots of the empirical
40
41 631 chronogram (Fig. 5a) and the mass extinction models (Fig. 6a,b). The age of the
42
43 632 reconstructed phylogenies was also considerably older than in mass extinction simulations,
44
45 633 especially for the 95% background extinction model (Fig. 6c,d; Appendix S11-S12). Several
46
47 634 of the reconstructed phylogenies under the high relative extinction model ($a = 0.95$) exhibited
48
49 635 a “broom-and-handle” shape (Appendix S12), and their LTT plots show a long period of no
50
51 636 growth ending in an upturn in the lineage accumulation curve (Fig. 6d). However, there was
52
53
54
55
56
57
58
59
60

1
2
3 637 usually no period of initial diversification and the average LTT plot was not anti-sigmoid
4
5 638 (Fig. 6d).

6
7
8 639

9
10 640 DISCUSSION

11
12 641 *Phylogenetic Relationships and Classification*

13
14
15 642 Our analysis confirms the monophyly of all four Chloranthaceae genera and corroborates
16
17 643 the relationships among genera recovered in previous studies (Eklund et al. 2004; Zhang and
18
19 644 Renner 2003). Nevertheless, it partially rejects the traditional intra-generic classification for
20
21 645 *Hedyosmum* proposed by Todzia (1988) based on morphological characters: subgenus
22
23 646 *Hedyosmum* and sections *Orientele*, *Macrocarpa*, and *Microcarpa* are shown to be
24
25 647 paraphyletic. Whether these sections should be abandoned or redefined should become clear
26
27 648 with the addition of more species in subgenus *Tafalla*, in particular, those from the informally
28
29 649 recognized group *Pseudoandromeda* (Todzia 1988), which were placed as sister to
30
31 650 *Macrocarpa* in Eklund et al. (2004).

32
33
34 651 The phylogenetic position of the enigmatic Asian endemic *H. orientale* has been under
35
36 652 debate. In Zhang and Renner's (2003) phylogenetic tree based on chloroplast DNA sequences
37
38 653 of five *Hedyosmum* species, *H. orientale* appeared as sister to all other *Hedyosmum* species.
39
40 654 Then, the morphological analysis by Eklund et al. (2004) indicated a placement as sister to *H.*
41
42 655 *grisebachii*, with the two species sister to *H. nutans* – a result more consistent with the
43
44 656 classification and cladistic analysis based on morphology by Todzia (1988). Indeed, in the
45
46 657 analysis performed by Eklund et al. (2004), constraining *H. orientale* to be sister to all other
47
48 658 *Hedyosmum* generated a tree that was two steps longer than the most parsimonious one, and
49
50 659 no morphological characters unequivocally supporting such placement could be identified.
51
52 660 However, the low node support meant that they could not place the species with confidence.
53
54 661 Our molecular phylogeny places *Hedyosmum orientale* as the sister clade to subgenus
55
56
57
58
59
60

Antonelli and Sanmartín, *Spatiotemporal evolution of Hedyosmum* Page 28 (51)

1
2
3 662 *Tafalla*, which is recognized here as monophyletic. Unfortunately, several attempts to
4
5 663 sequence the *rps16* intron of *Hedyosmum orientale* failed, but ITS data alone contained
6
7
8 664 strong phylogenetic signal for the placement suggested here (98% BS, 99% BP, Fig. 1).
9

10 665

11
12
13 666 *Spatiotemporal Evolution of Chloranthaceae*

14
15 667 Both parsimony-based and parametric ancestral area reconstructions (Fig. 3b, Fig. 4)
16
17 668 suggest that the most recent common ancestor (MRCA) of Chloranthaceae was already
18
19 669 distributed in America and Asia by the Early Cretaceous (~110 Ma). Australasia (area H) is
20
21
22 670 here interpreted as Asia, since *Chloranthus*, *Sarcandra*, and *Hedyosmum orientale* are
23
24
25 671 restricted to East Asia, while the presence of *Ascarina* in the Australian region and
26
27 672 Madagascar is probably the result of more recent dispersal events (Raven and Axelrod 1974;
28
29 673 Zhang and Renner 2003). This reconstruction agrees well with previous hypotheses (Raven
30
31 674 and Axelrod 1974; Todzia 1988), according to which Chloranthaceae originated in Laurasia
32
33
34 675 (North America and Eurasia) in the Early Cretaceous, diversified into the lineages leading to
35
36 676 the four extant genera, and then the *Hedyosmum* lineage dispersed to the Neotropics where it
37
38
39 677 radiated into its present-day diversity. A widespread Laurasian ancestor of Chloranthaceae is
40
41 678 also supported by the extensive fossil record of Chloranthaceae in the Holarctic (Zhang and
42
43
44 679 Renner 2003; Eklund et al. 2004). The oldest fossils of stem lineage *Hedyosmum* are from the
45
46 680 Barremian-Aptian of Portugal, and fossil pollen of *Asteropollis* (associated with *Hedyosmum*)
47
48
49 681 have been found in a wide range of localities in the Northern Hemisphere, including North
50
51 682 America, Greenland, and Europe. A similar Laurasian origin has been postulated for the
52
53 683 Asian genus *Chloranthus*, based on the presence of fossils of stem relatives in the Late
54
55 684 Cretaceous of North America and Europe (Eklund et al. 2004).

56
57
58 685 The nested position of *H. orientale* within the otherwise Neotropical crown group could
59
60 686 thus be a relict from a former widespread distribution in Laurasia (Todzia 1985). During the

1
2
3 687 Early Cenozoic, climate was wetter and more tropical and a boreotropical flora (Tiffney
4
5 688 1985) extended throughout the Northern Hemisphere from North America to Asia. Climatic
6
7
8 689 deterioration after the Eocene probably pushed boreotropical lineages south, and subsequent
9
10 690 extinction extirpated *Hedyosmum* lineages from Europe and North America, leaving behind
11
12 691 the Asian *H. orientale* as a relict. This hypothesis is supported by the LAGRANGE
13
14 692 reconstruction (Fig. 4), which shows the ancestor of crown group *Hedyosmum* originally
15
16 693 distributed in America and Asia in the Early Cenozoic (35.6 or 43.3 Ma, Table 1), where it
17
18 694 split into an exclusively American clade (the Antillean *H. nutans* – *H. grisebachii* clade) and
19
20 695 an Asian-American lineage, the *H. orientale-Tafalla* group. A key point in our biogeographic
21
22 696 scenario is the phylogenetic position of *H. orientale*. Placing this species as the sister clade of
23
24 697 the remaining species of *Hedyosmum*, as in Zhang and Renner 2003, would result in Asia
25
26 698 been inferred as the ancestral area of the genus in Lagrange and Fitch Parsimony.

27
28
29 699 Diversification tests and comparison between simulated and empirical phylogenies give
30
31 700 support to the hypothesis that high extinction rates, either punctual or constant (gradual),
32
33 701 have been responsible for the low extant diversity of Chloranthaceae relative to its old age
34
35 702 (65 species and 110 Ma). ML estimates of background extinction under a constant-rate model
36
37 703 were high ($a = 0.82$, Chloranthaceae) or very high ($a = 0.999$, *Hedyosmum* stem clade).
38
39 704 MEDUSA also estimated a high background extinction rate ($a = 0.78$) for the backbone of
40
41 705 the Chloranthaceae phylogeny, except for the branch leading to the South American
42
43 706 *Hedyosmum* Tafalla clade. Both high relative extinction rates (Rabosky and Lovette 2008)
44
45 707 and punctual mass extinction events (Cook and Crisp 2009) may produce a pattern of lineage
46
47 708 accumulation in which there is an excess of lineages close to the present, detected by the
48
49 709 gamma statistics as an increase in diversification rates (Table 2). Cook and Crisp (2009)
50
51 710 argued that the Terminal Eocene Event - the dramatic cooling of global climates at the
52
53 711 Eocene-Oligocene boundary - was responsible for the anti-sigmoid LTT plot and “broom-

1
2
3 712 and-handle” shape observed in the phylogenies of several legume clades. The anti-sigmoid
4
5 713 shape of the Chloranthaceae LTT plot resembles the 35 Ma simulated mass extinction model,
6
7
8 714 in that the end of the plateau, marking the initial recovery of lineage diversification, falls
9
10 715 around 35 Ma. High background extinction in the Holarctic, associated with subsequent
11
12 716 episodes of cooling and drying starting in the Oligocene (as modeled in the second part of the
13
14
15 717 35 Ma model), could further explain the very low extant diversity of Chloranthaceae,
16
17 718 especially in the Eastern Asian genera *Chloranthus* and *Sarcandra*, and perhaps in the
18
19 719 *Hedyosmum orientale* lineage.

20
21
22 720 There are, however, some problems with this mass extinction scenario. First, a 95% mass
23
24 721 extinction event in plants seems unrealistic. Nichols (2007) argued that about one third of all
25
26 722 angiosperm taxa in North America represented by fossil pollen failed to survive the impact
27
28
29 723 winter at the K/T event, including some 80% of all large plant species. Second, our
30
31 724 simulations assume that mass extinction events affect all lineages equally, but McLoughlin et
32
33
34 725 al. (2008) showed that the influence of the K/T event was minor in higher latitudes in the
35
36 726 Southern and Northern Hemispheres compared with the tropical regions nearer the impact.
37
38 727 Also, comparison of the shape of LTT plots from reconstructed phylogenies is not enough to
39
40 728 discriminate between mass extinction and high relative extinction scenarios, particularly
41
42 729 when faced with incomplete taxon sampling. Although the average LTT plot differs between
43
44 730 both scenarios (Fig. 6a-c), some of the 100 reconstructed phylogenies simulated under the
45
46 731 95% relative extinction model exhibited a “broom-and-handle” shape and long temporal gaps
47
48
49 732 between stem and crown ages that were similar to the observed Chloranthaceae chronogram.
50
51
52 733 Moreover, incomplete taxon sampling apparently causes a delay between the time of the
53
54 734 mass extinction event and the start of lineage recovery in the LTT plot of the reconstructed
55
56
57 735 extant phylogeny, which makes it difficult to discriminate between the alternative mass
58
59 736 extinction scenarios (65 Ma-35 Ma) using the LTT plot alone.

1
2
3 737
4
5
6 738 *Colonization of South America*
7
8 739 According to the Fitch and LAGRANGE reconstructions, the Neotropical region did
9
10 740 not form part of the ancestral distribution of *Hedyosmum*, but was instead the result of a more
11
12 741 recent colonization event, either at the divergence of subgenus *Tafalla* (Fig. 3a) or at the first
13
14 742 split in the *H. parvifolium-spectabile* clade within the *Tafalla* group (Fig. 4). The inclusion of
15
16 743 South America into the *Hedyosmum* ancestral distribution in the Bayes-DIVA analysis (Fig.
17
18 744 3b) is probably a result of DIVA cost assignments, which favor vicariance over dispersal, and
19
20 745 to the uncertainty in ancestral area reconstructions towards the root (Ronquist, 1997). In fact,
21
22 746 if the maximum number of areas in DIVA is constrained to two (maxareas = 2), Asia (H),
23
24 747 alone or together with West Indies (BH), is inferred as the ancestral area of Chloranthaceae,
25
26 748 and the West Indies (B) or West Indies-Asia (BH) as the geographic origin of *Hedyosmum*,
27
28 749 just as in the LAGRANGE analysis.
29
30
31
32
33
34 750 Based on Late Eocene divergence times, Zhang and Renner (2003) suggested that
35
36 751 *Hedyosmum* entered South America from the north following the same boreotropical route as
37
38 752 several other plant families (e.g. Moore and Donoghue 2007; Antonelli et al. 2009; Erkens et
39
40 753 al. 2009). Eklund et al. (2004) suggested the uplift of the Panama Isthmus (~3.5 Ma) as one
41
42 754 possible route for the dispersal of *Hedyosmum* into South America. Our temporal
43
44 755 reconstruction agrees better with Zhang and Renner's (2003) hypothesis: the MRCA of all
45
46 756 South American species (from *H. costaricense* to *H. racemosum*) is dated to the Miocene
47
48 757 (mean 15.2 Ma in PL, 19.4 Ma in BEAST; see Appendix S4–S7), long pre-dating the final
49
50 758 uplift of the Panama Isthmus. *Hedyosmum* might have entered South America via the
51
52 759 postulated Eocene-Oligocene Greater Antilles – Aves Ridge landbridge or the Late Miocene
53
54 760 island chain system, as a stepping-stone route (Iturralde-Vinent and MacPhee 1999).
55
56
57
58
59
60

1
2
3 761 Temporal-based diversification tests (LASER) indicate a significant increase in
4
5
6 762 diversification rates in the last 20 million years, largely coincident with the entrance of
7
8 763 *Hedyosmum* into South America (Figs. 3a, 4). MEDUSA also detects a significant
9
10 764 acceleration along the branch leading to the South American clade of *Hedyosmum*, subgenus
11
12 765 *Tafalla*. What triggered this acceleration in diversification in South American *Hedyosmum*?
13
14
15 766 The time of entrance into South America – estimated at ~17 Ma in Fitch (Fig. 3a) and ~15
16
17 767 Ma in LAGRANGE (Fig. 4) – occurred just at the onset of the most intense mountain uplift
18
19 768 phase in the Northern Andes (Gregory-Wodzicki 2000; Hoorn et al. 2010). This was also
20
21 769 during a period of global temperature optimum (the Middle Miocene Climatic Optimum),
22
23 770 followed by a period of increasing cooling (Zachos et al. 2001; Fig 3b). Any of these events,
24
25 771 individually or in combination, could have fostered speciation in *Hedyosmum*. The maximum
26
27 772 species diversity of *Hedyosmum* is found today in cool and moist environments of the
28
29 773 Neotropics, especially in the foothills of the Andes and the Central American cordilleras
30
31 774 (Appendix S1). Intuitively, it would therefore be natural to presume that climate cooling
32
33 775 played an important role in fostering diversification, by causing ecological shifts that
34
35 776 increased the occurrence of cooler habitats. Nevertheless, the Miocene–Pliocene climatic
36
37 777 cooling is now thought to have mainly affected lowland forests, by decreasing overall rainfall
38
39 778 and thus causing an expansion of arid and semi-arid habitats (Morley 2000). Previous studies
40
41 779 have shown that *Hedyosmum* cannot survive lowland drought, mainly due to the high
42
43 780 vulnerability of its xylem (Feild and Arens 2007). Put together, these lines of evidence
44
45 781 suggest that Neogene climatic cooling has not lead to a substantial expansion of habitats
46
47 782 suitable for the diversification of *Hedyosmum*.

55 783 Instead, it appears more likely that speciation in South American *Hedyosmum* was
56
57 784 triggered by the rapid formation of new montane regions during the uplift of the northeastern
58
59 785 Andes in the Middle Miocene onwards, and the habitat fragmentation that would result (Fig.

1
2
3 786 3b inset, yellow box). This scenario seems biologically plausible and has been proposed for
4
5 787 several other plant groups, such as in families Rubiaceae (Antonelli et al. 2009),
6
7
8 788 Valerianaceae (Bell and Donoghue 2005), Fabaceae (Hughes and Eastwood 2006), as well as
9
10 789 for animal groups, such as antbirds in the genus *Thamnophilus* (Brumfield and Edwards
11
12 790 2007). Continual uplift of highland regions could provide ongoing opportunities for
13
14
15 791 speciation via allopatric isolation and availability of new ecological niches (ecological
16
17 792 displacement). Indeed, Moore and Donoghue (2007) argued that dispersal of lineages into
18
19 793 new biogeographic regions (range evolution) is a main factor promoting shifts in rates of
20
21
22 794 diversification of plant lineages. Interestingly, this scenario is supported by our
23
24 795 biogeographic reconstructions: both Fitch Parsimony and Bayes-DIVA (Fig. 3) and
25
26 796 LAGRANGE (Fig. 4) indicate that most lineages in subgenus *Tafalla* diversified in the
27
28 797 Northern Andes (area C, alone or in conjunction with surrounding areas) throughout the
29
30 798 Neogene, from which they dispersed to the Central Andes (area D) and other regions. This is
31
32 799 also supported by paleobotanical findings of *Hedyosmum* fossil pollen (*Clavainaperturites*
33
34 800 *microclavatus*). Fossil records from the Early Miocene to the Early/Middle Miocene have
35
36 801 been retrieved from Santa Teresa in Peru, where it was common in montane forests but with
37
38 802 occasional occurrences in lowland forests (Hoorn 1994), and from the Late Miocene/Early
39
40 803 Pliocene onwards in Brazilian Amazonia (Silva-Caminha et al. 2010). It is believed that the
41
42 804 pollen grains found in lowland areas were produced in the Andean foothills and subsequently
43
44 805 transported by wind or water currents to their final deposition site (Hoorn 1994).
45
46
47
48
49

50 806 In contrast, neither the biological corridor created by the uplift of the Panama Isthmus nor
51
52 807 Pleistocene climatic changes – which earlier works hypothesized to have had a profound
53
54 808 impact on South American speciation (Haffer 1969; Gentry 1982) – seem to have played an
55
56 809 important role in the diversification of *Hedyosmum*. Most lineage splitting events are
57
58 810 estimated before the establishment of the Central American land bridge and before the onset
59
60

1
2
3 811 of Quaternary glaciations (Fig. 3b, inset). This result corroborates the inference that most
4
5 812 Neotropical diversification took place earlier in the Neogene (Hoorn et al. 2010).

6
7
8 813 Although diversification rates in the South American *Tafalla* clade were high ($r = 0.125$)
9
10 814 compared with the low rates in the rest of the tree ($r = 0.014$; MEDUSA), one cannot speak
11
12 815 here of a rapid adaptive radiation such as the one observed in the highland Neotropical genus
13
14 816 *Lupinus* (Hughes and Eastwood 2007). The empirical LTT plot of crown group *Hedyosmum*
15
16 817 did not significantly differ from a classic 2:1 birth-death model (Fig. 5c), and ML estimates
17
18 818 of speciation rates were not especially high: 0.080 lineages per million years for the crown
19
20 819 group (Table 2), or 0.286 in the *Hedyosmum Tafalla*-group. Again, our taxon sampling here
21
22 820 only represents half of extant species of *Hedyosmum*, and it is possible that adding the
23
24 821 missing species could increase speciation rates. Nevertheless, based on current evidence, it
25
26 822 seems that the sharp upturn in the lineage cumulative curve observed in the LTT plot of
27
28 823 Chloranthaceae is the result of both an increase in speciation rates in subgenus *Tafalla* and
29
30 824 high relative extinction rates in the remainder of the phylogeny.
31
32
33
34
35
36
37
38

39 826 *Correlates of Speciation and Extinction*

40
41 827 This study shows the advantages of combining paleontological, biogeographic,
42
43 828 molecular, and diversification data for reconstructing the history of a “relict”, species-poor
44
45 829 lineage, for which the extant diversity today is only a remnant of its past diversity. It also
46
47 830 points out the difficulties of inferring patterns of lineage diversification when incomplete
48
49 831 taxon sampling is combined with high extinction rates.
50
51
52

53 832 Cusimano and Renner (2010) demonstrated that using null distributions of randomly-
54
55 833 pruned trees to account for incomplete taxon sampling in empirical phylogenies – as in the
56
57 834 MCCR test and our TreeSim simulations – can lead to overestimating the probability of
58
59 835 departure from constant-rate diversification models. This is because actual taxon sampling is
60

1
2
3 836 rarely random, but often phylogenetically overdispersed – i.e., one representative per clade or
4
5
6 837 lineage is used, so that basal, early-diverging lineages are more likely to be represented in the
7
8 838 phylogeny than more recently diverged lineages. This effect is larger when testing decreasing
9
10 839 rates through time because internal nodes near the root leave more descendants and are more
11
12 840 likely to be included in a small taxon sample (Pybus & Harvey 2000; Cusimano and Renner
13
14
15 841 2010). In our study, we focused on increasing rates through time and our taxon sampling is
16
17 842 likely to be under-dispersed, since the aim was to sequence all available species of
18
19 843 *Hedyosmum*, but rarity led to some species not being included. Thus, our sampling is more
20
21 844 likely to have led to error Type II, i.e., erroneously accepting the null hypothesis of constant
22
23 845 rate diversification instead of changing diversification rates.
24
25

26
27 846 Many studies have focused on testing decreasing rates through time (Rabosky et al.
28
29 847 2007; Rabosky & Lovette 2008; Rabosky 2009). Increasing rates through time, as explored
30
31 848 here, is more difficult to test because both high background extinction and increasing
32
33 849 speciation rates can produce a pattern in which there is an excess of lineages close to the
34
35 850 present, translated into significantly positive gamma values. Birth-death likelihood models
36
37 851 can potentially distinguish between these two scenarios (Rabosky 2006b), but the power of
38
39 852 these tests is only high if the shift in diversification rate is large and the extinction fraction
40
41 853 moderately low ($a = 0.5$). Moreover, Rabosky (2009; 2010) demonstrated that the extinction
42
43 854 fraction cannot be reliably estimated from extant phylogenies with current diversification
44
45 855 methods because they either assume that rates have been constant among lineages (Pybus &
46
47 856 Harvey 2000; Rabosky 2006b) or they have been constant through time within clades
48
49 857 (Rabosky et al. 2007; Alfaro et al. 2009). This can lead to overestimation of extinction rates
50
51 858 from reconstructed extant phylogenies (Rabosky 2010). Estimators of background extinction
52
53 859 rates based on the relationship between clade age and species richness, as in the MEDUSA
54
55 860 approach, can be especially misleading in comparisons across higher taxa because it assumes
56
57
58
59
60

1
2
3 861 that there are no ecological limits to a clade's increase in diversity or "carrying capacity"
4
5 862 (Rabosky 2009). One way to improve estimates is to incorporate fossil taxa directly into
6
7
8 863 diversification analyses (Quental & Marshall 2010; Rabosky 2010). For example, including
9
10 864 fossil stem lineages in the phylogeny (e.g., as done by Eklund et al. 2004) could improve
11
12 865 reliable estimation of diversification rates and help reduce the uncertainty in ancestral area
13
14
15 866 estimation for the deepest nodes in Chloranthaceae.

16
17 867 In general, and given that a wide range of processes can give similarly shaped
18
19 868 reconstructed phylogenies (Quental & Marshall 2010), it is important to merge additional
20
21 869 sources of information such as the fossil record or the inference of biogeographic ranges to
22
23 870 analyses of diversification. For Chloranthaceae, both the fossil record and biogeographic
24
25 871 inference give support to the hypothesis that the ancestor of Chloranthaceae was widespread
26
27 872 in Laurasia and that current low extant diversity is the result of gradual extinction. It also
28
29 873 shows how old groups such as Chloranthaceae, which apparently have reached their
30
31 874 equilibrium diversity (Rabosky 2009), can increase their "carrying capacity" through
32
33 875 invasion of new biogeographic regions or ecological niches – in this case the colonization of
34
35 876 the tropical Andes.

36
37
38
39
40
41 877

42 43 878 **FUNDING**

44
45 879 A.A. was funded by grants from the Swedish Research Council, the Royal Swedish Academy
46
47 880 of Sciences, Royal Society of Arts and Sciences in Göteborg, Kungliga och Hvitfeldtska
48
49 881 Stiftelsen, Helge Ax:son Johnsons Stiftelse, Göteborg University, and Carl Tryggers Stiftelse.
50
51 882 I.S was funded by the Spanish Ministry of Education and Science through the program
52
53 883 "Ramon y Cajal" and research grant (CGL2009-13322-C03-0), and by NESCent (US NSF
54
55 884 #EF-0423641).

56
57
58
59
60 885

886 **ACKNOWLEDGEMENTS**

887 We warmly acknowledge J. Doyle, T. Feild, C. Persson, T. Sempere, R. Eriksson, S. Silva, E.
888 Paradis, D. Rabosky, A. Rambaut, and B Oxelman for fruitful discussions and various help at
889 different stages of this study; R. Abbott for field samples; D. Santamaría, N. Zamora, L.
890 Kinoshita, A. Herrera, C. Galdames, and M. Correa for assistance during fieldwork; V. Aldén
891 for laboratory assistance. Special thanks to Tanja Stadler for help with TreeSim, Sven Buerki
892 for help with BEAST and comments on the manuscript, and to Joel Cracraft and Michael
893 Donoghue for inspiring discussions at NESCENT. This manuscript has been considerably
894 improved thanks to the constructive criticism and suggestions from J. Sullivan, S. Renner,
895 and three anonymous reviewers.

896 **REFERENCES**

- 897 Alfaro M.E., Santini F., Brock C., Alamillo H., Dornburg A., Rabosky D.L., Carnevale G.,
898 Harmon L.J. 2009. Nine exceptional radiations plus high turnover explain species
899 diversity in jawed vertebrates. *Proc. Natl. Acad. Sci. USA.* 106:13410-13414.
- 900 Antonelli A. 2008. Higher level phylogeny and evolutionary trends in Campanulaceae
901 subfam. Lobelioideae: Molecular signal overshadows morphology. *Mol. Phlogenet.*
902 *Evol.* 46:1-18.
- 903 Antonelli A., Nylander J.A.A., Persson C., Sanmartín I. 2009. Tracing the impact of the
904 Andean uplift on Neotropical plant evolution. *Proc. Natl. Acad. Sci. USA.* 106:9749-
905 9754.
- 906 Bell C.D., Donoghue M.J. 2005. Phylogeny and biogeography of Valerianaceae (Dipsacales)
907 with special reference to the South American valerians. *Org. Divers. Evol.* 5:147-159.
- 908 Britton T. 2005. Estimating Divergence Times in Phylogenetic Trees Without a Molecular
909 Clock. *Syst. Biol.* 54:500-507.
- 910 Brumfield R.T., Edwards S.V. 2007. Evolution into and out of the Andes: A Bayesian
911 analysis of historical diversification in *Thamnophilus* antshrikes. *Evolution* 61:346-
912 367.
- 913 Crisp M.D., Cook L.G. 2009. Explosive radiation of cryptic mass extinction? Interpreting
914 signatures in molecular phylogenies. *Evolution* 63:2257-2265.
- 915 Cusimano N., Renner S.S. 2010. Slowdowns in diversification rates from real phylogenies
916 may not be real. *Syst. Biol.*, 59:458-464.
- 917 Dahlgren R. 1983. General aspects of angiosperm evolution and macrosystematics. *Nord. J.*
918 *Bot.* 3:119-149.

- 1
2
3 919 Doyle J.A., Eklund H., Herendeen P.S. 2003. Floral evolution in Chloranthaceae:
4
5 920 Implications of a morphological phylogenetic analysis. *Int. J. Plant Sci.* 164:S365-
6
7
8 921 S382.
9
10 922 Doyle J.A., Endress P. K. 2000. Morphological Phylogenetic Analysis of Basal Angiosperms:
11
12 923 Comparison and Combination with Molecular Data. *Int. J. Plant Sci.* 161:S121-S153.
13
14
15 924 Drummond A.J., Ho S.Y.W., Phillips M.J., Rambaut A. 2006. Relaxed phylogenetics and
16
17 925 dating with confidence. *PLoS Biol.* 4:699-710.
18
19
20 926 Drummond A.J., Rambaut A. 2007. BEAST: Bayesian evolutionary analysis by sampling
21
22 927 trees. *Bmc Evol. Biol.* 7:8.
23
24
25 928 Eklund H., Doyle J.A., Herendeen P.S. 2004. Morphological phylogenetic analysis of living
26
27 929 and fossil Chloranthaceae. *Int. J. Plant Sci.* 165:107-151.
28
29
30 930 Endress P. K., Doyle J.A. 2009. Reconstructing the ancestral angiosperm flower and its initial
31
32 931 specializations. *Am. J. Bot.* 96:22-66.
33
34
35 932 Erkens R.H.J., Maas J.W., Couvreur T.L.P. 2009. From Africa via Europe to South America:
36
37 933 migrational route of a species-rich genus of Neotropical lowland rain forest trees
38
39 934 (*Guatteria*, Annonaceae). *J. Biogeogr.* 36:2338-2352.
40
41
42 935 Feild T.S., Arens N.C. 2007. The ecophysiology of early angiosperms. *Plant Cell Environ.*
43
44 936 30:291-309.
45
46
47 937 Friis E.M., Crane P.R., Pedersen K.R. 1997. Fossil history of magnoliid angiosperms. In
48
49 938 Iwatsuki K., Raven P.H. *Evolution and diversification of land plants*:121–156.
50
51
52 939 Friis E.M., Pedersen K.R., Crane P. R. 1994. Angiosperm floral structures from the Early
53
54 940 Cretaceous of Portugal. *Plant Syst. Evol.* 8:31–50.
55
56
57 941 Gentry A.H. 1982. Neotropical floristic diversity: phytogeographical connections between
58
59 942 Central and South America, Pleistocene climatic fluctuations, or an accident of the
60
943 Andean orogeny? *Ann. Mo. Bot. Gard.* 69:557-593.

Antonelli and Sanmartín, *Spatiotemporal evolution of Hedyosmum* Page 40 (51)

- 1
2
3 944 Gradstein F.M., Ogg J.G., Smith A. G. 2005. A Geologic Time Scale 2004. In Gradstein
4
5 945 F.M., Ogg J.G. A Geologic Time Scale 2004. Cambridge University Press.
6
7
8 946 Gregory-Wodzicki K.M. 2000. Uplift history of the Central and Northern Andes: A review.
9
10 947 Bull. Geol. Soc. Am. 112:1091-1105.
11
12 948 Haffer J. 1969. Speciation in amazonian forest birds. Science 165:131-137.
13
14
15 949 Harmon L.J., Weir J.T., Rock C.D., Glor R.E., Challenger W. 2003. GEIGER: investigating
16
17 950 evolutionary radiations. Bioinformatics, 24:129-131.
18
19
20 951 Hartmann K., Wong D., Stadler T. 2010. Sampling Trees from Evolutionary Models. Syst.
21
22 952 Biol., 59:465-476.
23
24 953 Harvey P.H., May R.M., Nee S. 1994. Phylogenies without fossils. Evolution, 48:523-529.
25
26
27 954 Herendeen, P.S., Crepet W.L., Nixon K.C. 1993. *Chloranthus*-like stamens from the Upper
28
29 955 Cretaceous of New Jersey. Am. J. Bot. 80:865-871.
30
31
32 956 Hochuli P.A., Heimhofer U., Weissert H. 2006. Timing of early angiosperm radiation:
33
34 957 recalibrating the classical succession. Geol. Soc. Lond. 163:587-594.
35
36 958 Hoorn C. 1994. An environmental reconstruction of the palaeo-Amazon River System
37
38 959 (Middle-Late Miocene, NW Amazonia). Palaeogeogr. Palaeoclimatol. Palaeoecol.
39
40 960 112:187-238.
41
42
43 961 Hoorn C., Wesselingh F.P., Steege H. ter, Bermudez M.A., Mora A., Sevink J., Sanmartín I.,
44
45 962 Sanchez-Meseguer A., Anderson C. L., Figueiredo J.P. *et al.*.2010. Amazonia
46
47 963 Through Time: Andean Uplift, Climate Change, Landscape Evolution, and
48
49 964 Biodiversity. Science 330:927–931.
50
51
52 965 Huelsenbeck J.P., Ronquist F. 2001. MRBAYES: Bayesian inference of phylogenetic trees.
53
54 966 Bioinformatics 17:754-755.
55
56
57
58
59
60

- 1
2
3 967 Hughes C., Eastwood R. 2006. Island radiation on a continental scale: Exceptional rates of
4
5 968 plant diversification after uplift of the Andes. *Proc. Natl. Acad. Sci. USA.* 103:10334-
6
7 969 10339.
8
9
10 970 Iturralde-Vinent M.A., MacPhee R.D.E. 1999. Paleogeography of the Caribbean region:
11
12 971 implications for Cenozoic biogeography. *Bull. Am. Mus. Nat. Hist.* 238:1-95.
13
14
15 972 Katoh K., Asimenos G., Toh H. 2009. Multiple Alignment of DNA Sequences with MAFFT.
16
17 973 In Posada, D. *Bioinformatics for DNA Sequence Analysis*, p. 39-64. Springer
18
19 974 *Protocols*.
20
21
22 975 Kong H.Z., Chen Z.D., Lu A.M. 2002. Phylogeny of *Chloranthus* (Chloranthaceae) based on
23
24 976 nuclear ribosomal ITS and plastid TRNL-F sequence data. *Am. J. Bot.* 89:940-946.
25
26
27 977 Linder H.P., Hardy C.R., Rutschmann F. 2005. Taxon sampling effects in molecular clock
28
29 978 dating: An example from the African Restionaceae. *Mol. Phlogenet. Evol.* 35:569-
30
31 979 582.
32
33
34 980 Maddison W.P., Maddison D.R. 2007. Mesquite: a modular system for evolutionary analysis.
35
36 981 Version 2.01. Available at: mesquiteproject.org.
37
38
39 982 McLoughlin S., Carpenter R.J., Jordan G.J., Hill R.S. 2008. Seed ferns survived the end-
40
41 983 Cretaceous mass extinction in Tasmania. *Am. J. Bot.*, 95:465-471.
42
43
44 984 Moore B.R., Donoghue M.J. 2007. Correlates of diversification in the plant clade dipsacales:
45
46 985 Geographic movement and evolutionary innovations. *Amer. Nat.* 170:S28-S55.
47
48
49 986 Morley R.J. 2000. *Origin and evolution of tropical rain forests*. Wiley, New York.
50
51 987 Nee S., Mooers A., Harvey P.H. 1992. Tempo and mode of evolution revealed from
52
53 988 molecular phylogenies. *Proc. Natl. Acad. Sci. U.S.A.* 89:8322-83265
54
55
56 989 Nee S., Holmes E.C., May R.M., Harvey P.H. 1994a. Extinctions rates can be estimated from
57
58 990 molecular phylogenies. *Philos. Trans. R. Soc. Lond.* 344:77-82.
59
60

Antonelli and Sanmartín, *Spatiotemporal evolution of Hedyosmum* Page 42 (51)

- 1
2
3 991 Nee S., May R.M., Harvey P.H. 1994b. The reconstructed evolutionary process. *Philos.*
4
5 992 *Trans. R. Soc. Lond., B, Biol. Sci.* 344, 305–311
6
7
8 993 Nichols D.J. 2007. Selected plant microfossil records of the terminal Cretaceous event in
9
10 994 terrestrial rocks, western North America. *Palaeogeogr. Palaeoclimatol. Palaeoecol.*
11
12 995 255:22-34.
13
14
15 996 Nylander J.A.A. 2004. MrModeltest v2. Program distributed by the author. Evolutionary
16
17 997 Biology Centre, Uppsala University.
18
19
20 998 Nylander J.A.A., Wilgenbusch J.C., Warren D.L., Swofford D.L. 2008a. AWTY (are we
21
22 999 there yet?): a system for graphical exploration of MCMC convergence in Bayesian
23
24 1000 phylogenetics. *Bioinformatics.* 24:581-583.
25
26
27 1001 Nylander J. A. A., Olsson U., Alström P., Sanmartín I. 2008b. Accounting for Phylogenetic
28
29 1002 Uncertainty in Biogeography: A Bayesian Approach to Dispersal-Vicariance Analysis
30
31 1003 of the Thrushes (Aves: Turdus). *Syst. Biol.* 57:257-268.
32
33
34 1004 Paradis E., Claude J., Strimmer K. 2004. APE: Analyses of Phylogenetics and Evolution in R
35
36 1005 language. *Bioinformatics* 20:289-290.
37
38
39 1006 Pybus O.G., Harvey P.H. 2000. Testing macro-evolutionary models using incomplete
40
41 1007 molecular phylogenies. *Proc. R. Soc. Lond. B* 267:2267-2272.
42
43
44 1008 Qiu Y.L., Lee J., Bernasconi-Quadroni F., Soltis D.E., Soltis P.S., Zanis M., Zimmer E.A.,
45
46 1009 Chen Z., Savolainen V., Chase M.W. 2000. Phylogeny of Basal Angiosperms:
47
48 1010 Analyses of Five Genes from Three Genomes. *Int. J. Plant Sci.* 161:S3-S27.
49
50
51 1011 Quental T.B., C.R. Marshall. 2010. Diversity dynamics: molecular phylogenies need the
52
53 1012 fossil record. *TREE* 25:434-441.
54
55
56 1013 Rabosky D.L. 2006a. LASER: a maximum likelihood toolkit for detecting temporal shifts in
57
58 1014 diversification rates. *Evol. Bioinform. Online* 2:257-260.
59
60

- 1
2
3 1015 Rabosky D.L. 2006b. Likelihood methods for detecting temporal shifts in diversification
4
5 1016 rates. *Evolution* 60:1152-1164.
6
7
8 1017 Rabosky D.L. 2009. Ecological limits on clade diversification in higher taxa. *Am. Nat.*
9
10 1018 173:662-674.
11
12
13 1019 Rabosky D.L. 2010. Extinction rates should not be estimated from molecular phylogenies.
14
15 1020 *Evolution*, 64:1816-1824.
16
17 1021 Rabosky D.L., and I. J. Lovette. 2008. Explosive evolutionary radiations: Decreasing
18 1022 speciation or increasing extinction through time? *Evolution* 62:1866-1875.
19
20
21
22 1023 Rabosky D.L., Donnellan S.C., Talaba A.L., Lovette I.J. 2007. Exceptional among-lineage
23 1024 variation in diversification rates during the radiation of Australia's most diverse
24 1025 vertebrate clade. *Proc. R. Soc. B.* 274:2915-2923.
25
26
27
28
29 1026 Rambaut A. 2002. PHYLOGEN v. 1.1. Manual.
30
31 1027 Rambaut A. 2008. FigTree v1.1. Available from <http://tree.bio.ed.ac.uk/software/figtree>.
32
33
34 1028 Rambaut A., Drummond A.J. 2007. Tracer v1.4. Available from
35
36 1029 <http://beast.bio.ed.ac.uk/Tracer>.
37
38
39 1030 Raven P.H., Axelrod D.I. 1974. Angiosperm biogeography and past continental movements.
40
41 1031 *Ann. Mo. Bot. Gard.* 61:539-673.
42
43
44 1032 Ree R.H., Moore B.R., Webb C.O., Donoghue M.J. 2005. A likelihood framework for
45 1033 inferring the evolution of geographic range on phylogenetic trees. *Evolution*,
46
47 1034 59:2299-2311.
48
49
50
51 1035 Ree R.H., Sanmartín I. 2009. Prospects and challenges for parametric models in historical
52 1036 biogeographical inference. *J. Biogeogr.* 36:1211-1220.
53
54
55 1037 Ree R.H., Smith S.A. 2008. Maximum likelihood inference of geographic range evolution by
56 1038 dispersal, local extinction, and cladogenesis. *Syst. Biol.* 57:4-14.
57
58
59
60

Antonelli and Sanmartín, *Spatiotemporal evolution of Hedyosmum* Page 44 (51)

- 1
2
3 1039 Ronquist F. 1997. Dispersal-vicariance analysis: A new approach to the quantification of
4
5 1040 historical biogeography. *Syst. Biol.* 46:195-203.
6
7
8 1041 Ronquist F. 2001. DIVA 1.2. Computer programme distributed by the author. Available from
9
10 1042 <http://www.ebc.uu.se/systzoo/research/diva/diva.html>.
11
12
13 1043 Sanderson M.J. 2002. Estimating Absolute Rates of Molecular Evolution and Divergence
14
15 1044 Times: A Penalized Likelihood Approach. *Mol. Biol. Evol.* 19:101-109.
16
17
18 1045 Sanderson M.J. 2003. r8s: inferring absolute rates of molecular evolution and divergence
19
20 1046 times in the absence of a molecular clock. *Bioinformatics* 19(2):301-302.
21
22 1047 Sanmartin I. 2003. Dispersal vs. vicariance in the Mediterranean: Historical biogeography of
23
24 1048 the Palearctic Pachydeminae (Coleoptera, Scarabaeoidea). *J. Biogeogr.* 30:1883-1897.
25
26
27 1049 Sanmartin I. 2007. Event-based biogeography: Integrating patterns, processes, and time. In
28
29 1050 Ebach M.C., Tangney R. *Biogeography in a Changing World*, p. 135-159 Press-
30
31 1051 Taylor and Francis Group, Boca Raton.
32
33
34 1052 Silva-Caminha S.A.F., Jaramillo C.A., Absy M.L. 2010. Neogene palynology of the
35
36 1053 Solimões Basin, Brazilian Amazonia. *Palaeontographica Abt. B* 283:1-67.
37
38
39 1054 Stadler T. 2009. On incomplete sampling under birth-death models and connections to the
40
41 1055 sampling-based coalescent. *J. Theor. Biol.* 261:58-66.
42
43
44 1056 Stadler T. in press, 2011. Simulating trees on a fixed number of extant species. *Syst. Biol.*
45
46 1057 Swofford D.L. 2002. PAUP*: phylogenetic analysis using parsimony (* and other methods)
47
48 1058 Version 4.0b10.
49
50
51 1059 Tiffney B.H. 1985. Perspectives on the origin of the floristic similarity between eastern Asia
52
53 1060 and eastern North America. *J. Arnold Arbor.* 66:73-94.
54
55
56 1061 Todzia C.A. 1988. Chloranthaceae: Hedyosmum. *Flora Neotropica Monographies* 48:1-139.
57
58 1062 Todzia C.A. 1993. New Species of Hedyosmum (Chloranthaceae) from Northern South
59
60 1063 America. *Novon* 3:81-85.

- 1
2
3 1064 Weir J.T. 2006. Divergent timing and patterns of species accumulation in lowland and
4
5 1065 highland Neotropical birds. *Evolution* 60:842-855.
6
7 1066 Wijninga V.M. 1996. Palynology and paleobotany of the Early Pliocene section Rio Frio 17
8
9 1067 (Cordillera Oriental, Colombia): Biostratigraphical and chronostratigraphical
10
11 1068 implications. *Rev. Palaeobot. Palynol.* 92:329-350.
12
13 1069 Young K., Ulloa C., Luteyn J., Knapp S. 2002. Plant evolution and endemism in Andean
14
15 1070 South America: an introduction. *Bot. Rev.* 68:4-21.
16
17 1071 Yule G.U. 1924. A mathematical theory of evolution, based on the conclusions of Dr. JC
18
19 1072 Willis. *Philos. Trans. Roy. Soc. London Ser. B* 213:21-87.
20
21 1073 Zachos J., Pagani M., Sloan L., Thomas E., Billups K. 2001. Trends, rhythms, and
22
23 1074 aberrations in global climate 65 Ma to present. *Science* 292:686-693.
24
25 1075 Zanis M.J., Soltis D.E., Soltis P.S., Mathews S., Donoghue M.J. 2002. The root of the
26
27 1076 angiosperms revisited. *Proc. Natl. Acad. Sci. USA.* 99:6848.
28
29 1077 Zhang L.B., Renner S. 2003. The deepest splits in Chloranthaceae as resolved by chloroplast
30
31 1078 sequences. *Int. J. Plant Sci.* 164:S383-S392.
32
33 1079 Zwickl D.J. 2006. Genetic algorithm approaches for the phylogenetic analysis of large
34
35 1080 biological sequence datasets under the maximum likelihood criterion. Ph.D.
36
37 1081 dissertation, The University of Texas at Austin.
38
39
40
41
42
43
44
45
46
47
48
49
50
51
52
53
54
55
56
57
58
59
60

1082

1083 TABLE 1. Crown group ages of major clades in Chloranthaceae.

Clade	Penalized Likelihood		Bayesian relaxed clock			Zhang and Renner (2003)		
	Mean	95 % CI Lower	95 % CI Upper	Mean	95% HPD Lower	95% HPD Upper	“Fossil A”	“Fossil B”
Chloranthaceae	110	110	110	111.2	110	112	120	210–263*
<i>Ascarina</i>	14.5	4.79	44.8	12.8	3.37	25.1	(9 or 10)±6	(17 or 18)±13
<i>Sarcandra</i>	9.91	1.32	37.5	6.88	0.28	17.3	-	-
<i>Chloranthus</i>	33.0	20.4	72.4	36.2	20.8	55.0	11 or 12	22
<i>Hedyosmum</i>	35.6	25.9	43	43.3	30.1	57.1	29±11	(53 or 63)±20

1084 *Calculated by us from substitution rates and node-to-tip distances provided in the original

1085 article. CI, confidence interval; HPD, highest posterior density.

1086 TABLE 2. Results of fitting four rate-constant and rate-variable birth-death models to empirical chronograms.

Macro-evolutionary model	pure birth	birth death	yule-2-rate	yule-3-rate	Gamma statistic	$dAIC_{RC}$
					MCCR test (p value)	p value
Chloranthaceae	LH -48.083	LH -44.52	LH -40.98	LH -37.68	2.241	7.689
	AIC 98.166	AIC 93.043	AIC 87.95	AIC 85.35	$p > 0.999$ (critical value = -2.014)	$p < 0.001$
	$r = 0.0463$	$r = 0.0148$	$r_1 = 0.0148$	$r_1 = 0.0148$		
		$a = 0.82$	$r_2 = 0.0683$	$r_2 = 0.0799$		
			$st_1 = 23.291$	$r_3 = 0.0121$		
				$st_1 = 23.291$		
				$st_2 = 2.106$		
<i>Hedyosmum</i> stem lineage	LH -36.52	LH -31.93	LH -30.63	LH -28.14	2.554	1.587
	AIC = 75.05	AIC 67.87	AIC 67.27	AIC 66.28	$p > 0.999$	$p = 0.049$
	$r = 0.049$	$r = 3.98 \text{ e-}07$	$r_1 = 0.011$	$r_1 = 0.011$	(critical value = -1.885)	
		$a = 0.999$	$r_2 = 0.077$	$r_2 = 0.10$		
			$st_1 = 23.29$	$r_3 = 0.025$		
				$st_1 = 23.29$		

	$st_2 = 3.50$					
<i>Hedyosmum</i> crown group	LH -25.41	LH -25.41	LH -22.98	LH -21.93	-0.382	0.868
	AIC 52.83	AIC 54.83	AIC 51.96	AIC 53.85	$p = 0.7426$	$p = 0.099$
	$r = 0.080$	$r = 0.080$	$r_1 = 0.103$	$r_1 = 0.074$	(critical value = -2.089)	
		$a = 0$	$r_2 = 0.026$	$r_2 = 0.144$		
			$st_1 = 3.50$	$r_3 = 0.026$		
				$st_1 = 8.71$		
				$st_2 = 3.50$		

1087 Only observed branching times in the original chronogram were considered as branching points for the Yule-n-rate models. Abbreviations: $a =$
1088 extinction fraction (dlb); $r =$ diversification rate: speciation (b) – extinction (d); $r_1 =$ initial diversification rate; $r_2 - r_3 =$ final diversification rates;
1089 st_i : point in time when there is a shift in diversification rate. $dAIC_{RC}$ is the difference in Akaike information criterion (AIC) scores between the
1090 best rate-constant model (the one with the lowest AIC value) and the best rate-variable model. MCCR: Monte Carlo Constant rate test for the
1091 gamma statistic. P -values were derived from simulated trees generated under the pure birth model with the same number of lineages as the
1092 original phylogeny and using the estimated pure birth speciation values.

1093

1094 FIGURE CAPTIONS

1095 FIGURE 1. Phylogeny of *Hedyosmum*. The tree is the 50% majority-rule consensus from the
1096 MCMC Bayesian analysis, based on *rbcL*, *rps16*, and ITS. A thick-lined branch indicates that
1097 the branch was also present in the majority-rule consensus tree of the bootstrap analysis.
1098 Numbers above branches indicate the posterior probability of the clade. Numbers below
1099 branches show bootstrap support values, whenever applicable. Species names in bold indicate
1100 types for genera.

1102 FIGURE 2. Molecular chronogram of Chloranthaceae, estimated using Penalized Likelihood.
1103 The tree topology is the same as in Fig. 1, but with node ages calculated from mean branch
1104 lengths of 16,000 trees from the Bayesian stationary sample. Bars at node intersections
1105 indicate 95 % confidence intervals of ages, calculated by independently dating 1000 trees
1106 randomly sampled from the MCMC Bayesian stationary distribution. Minimal age constraints
1107 were established by two fossils: C₁, *Hedyosmum*-like female flowers from the Barremian-
1108 Aptian of Portugal (associated with *Asteropollis* pollen); C₂, *Chloranthus*-like stamens from
1109 the Late Cretaceous of New Jersey (*Chloranthistemon crossmanensis*). Note the gap of ~85
1110 Ma between the stem age of *Hedyosmum* and its inferred crown age; in the fossil record, this
1111 gap is about 100 Ma. Timescale from Gradstein (2005). Fossil images reproduced with
1112 permission (light microscopy of Miocene pollen: courtesy Silane Silva).

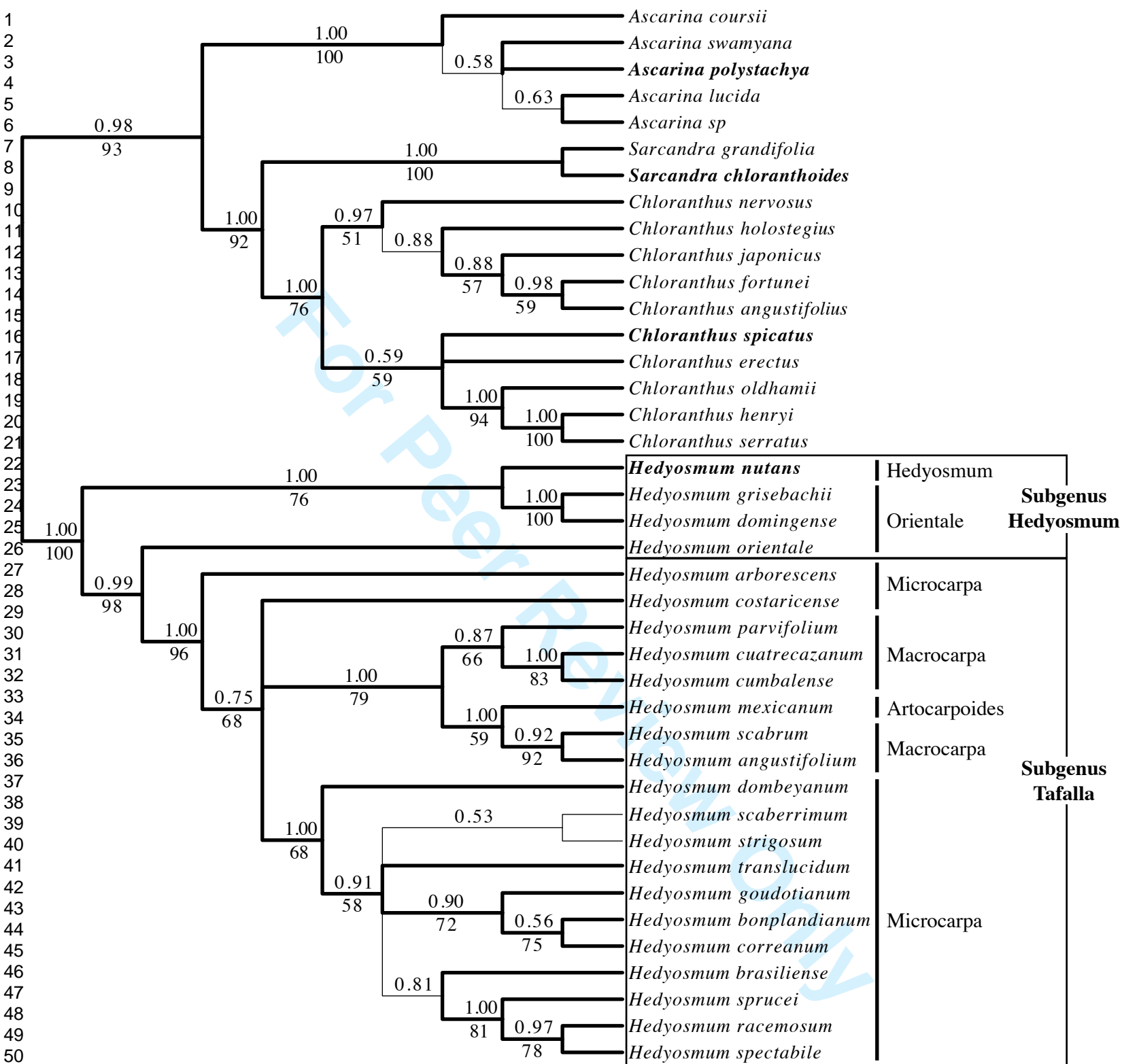
1114 FIGURE 3. Spatiotemporal reconstruction of Chloranthaceae, with special reference to
1115 *Hedyosmum*, inferred using *a*) Fitch parsimony and *b*) BAYES-DIVA. The tree is the 50%
1116 majority rule consensus from the MCMC Bayesian analysis. Pie charts at nodes show the
1117 probabilities of alternative ancestral area reconstructions obtained by integrating Fitch and
1118 DIVA optimizations over a distribution sample of trees from the Bayesian analysis ($N =$

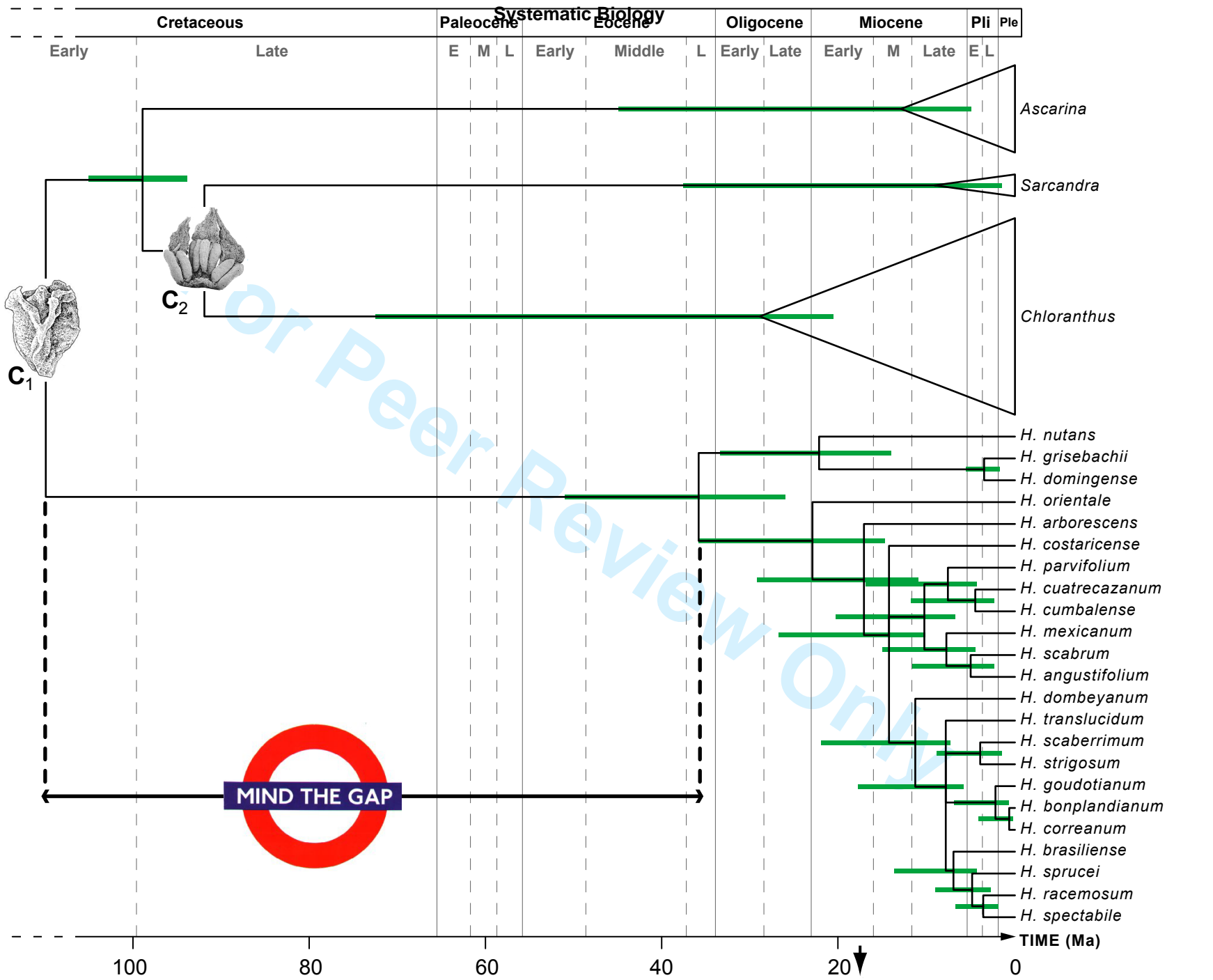
1
2
3 1119 1000); the first four areas with highest probability are colored according to their relative
4
5 1120 probability in the following order: white >red >blue >gray; any remaining areas and
6
7
8 1121 ambiguous reconstructions in the Fitch optimizations are collectively given in black. Current
9
10 1122 distributions are listed before each species. The red arrow indicates a significant shift in
11
12 1123 diversification rate (see text). *INSETS*: a) Operational areas used in the analysis (A: Central
13
14 1124 America, B: West Indies, C: Northern Andes, D: Central Andes, E: Chocó, F: Guiana Shield,
15
16 1125 G: Southeastern South America, H: Australasia; topographic map from the National
17
18 1126 Geophysical Data Center, www.ngdc.noaa.gov). b) Lineage through time (LTT) plot of
19
20 1127 *Hedyosmum*. The blue line represents the accumulation of lineages in the mean age
21
22 1128 chronogram of Figure 2. Uncertainty in age estimations is illustrated by 1000 individually
23
24 1129 dated chronograms (grey lines) randomly sampled from the Bayesian MCMC stationary
25
26 1130 distribution. Global temperature means are shown by the red curve (adapted from Zachos et
27
28 1131 al. 2001). The yellow box indicates the period of most intensive uplift in the Northern Andes
29
30 1132 (~ 15–5 Ma; Hoorn et al. 2010).
31
32
33
34
35
36
37
38

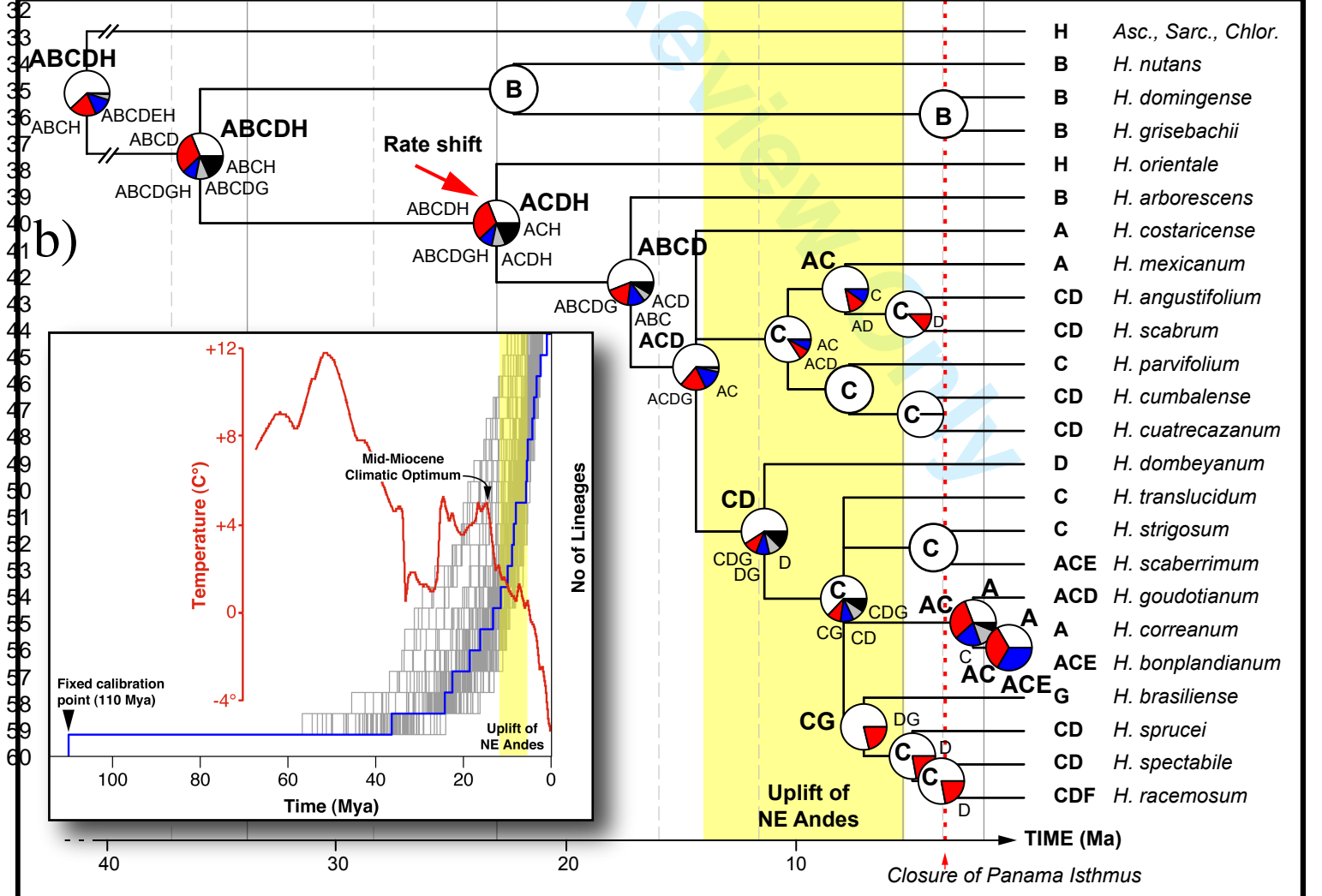
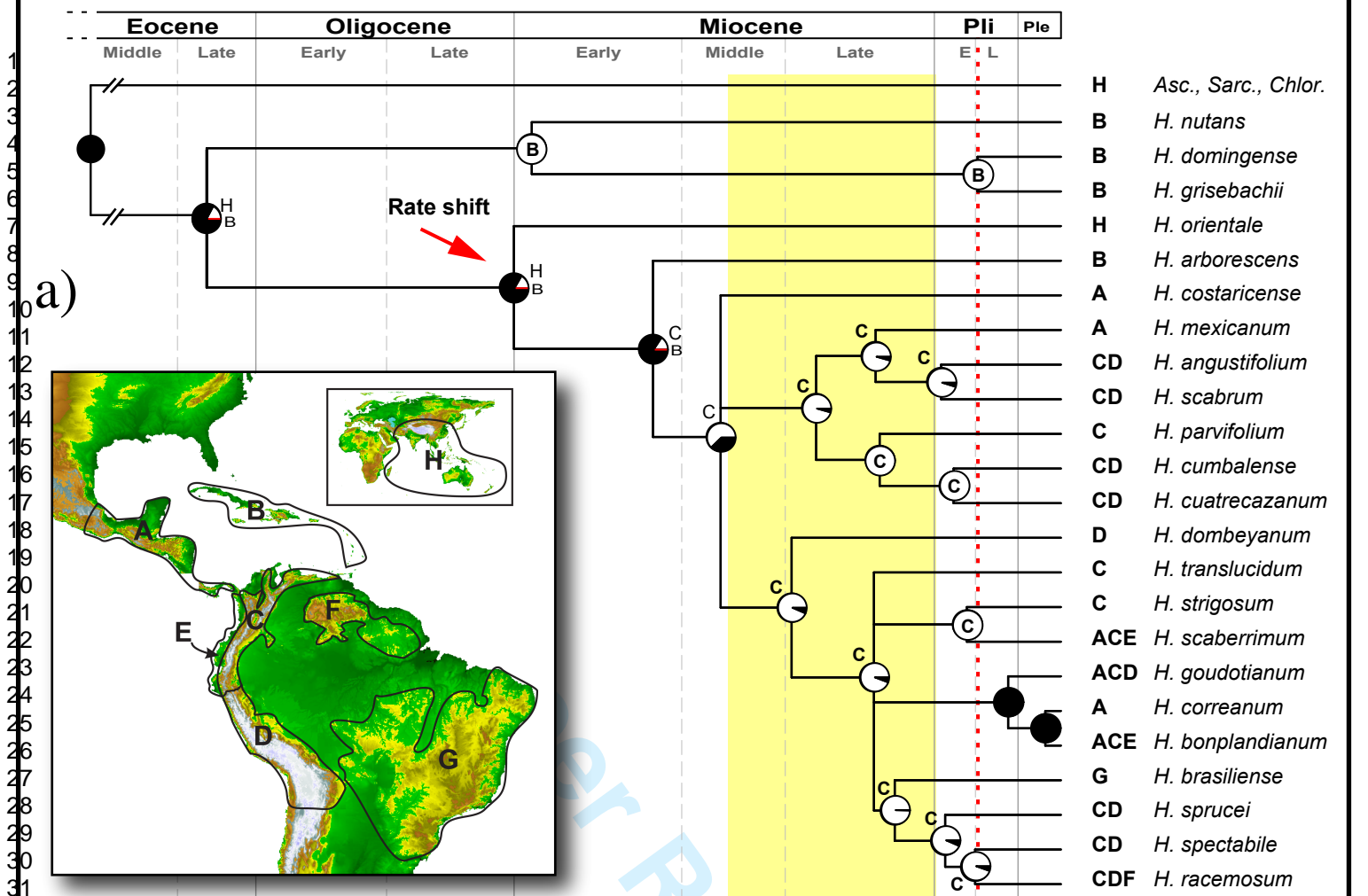
39 1134 FIGURE 4: Spatiotemporal reconstruction of Chloranthaceae inferred using the Dispersal-
40
41 1135 Extinction-Cladogenesis likelihood method implemented in LAGRANGE (Ree and Smith,
42
43 1136 2008). The tree is the ‘allcompat’ phylogram (50% majority rule with compatible groups
44
45 1137 added) from the MCMC Bayesian analysis with time-calibrated branch lengths estimated by
46
47 1138 penalized likelihood. Ancestral distributions were constrained to include only two-area
48
49 1139 ranges. Pie charts at nodes represent ML relative probabilities for ancestral areas. Other
50
51 1140 conventions as in Fig. 3.
52
53
54
55
56

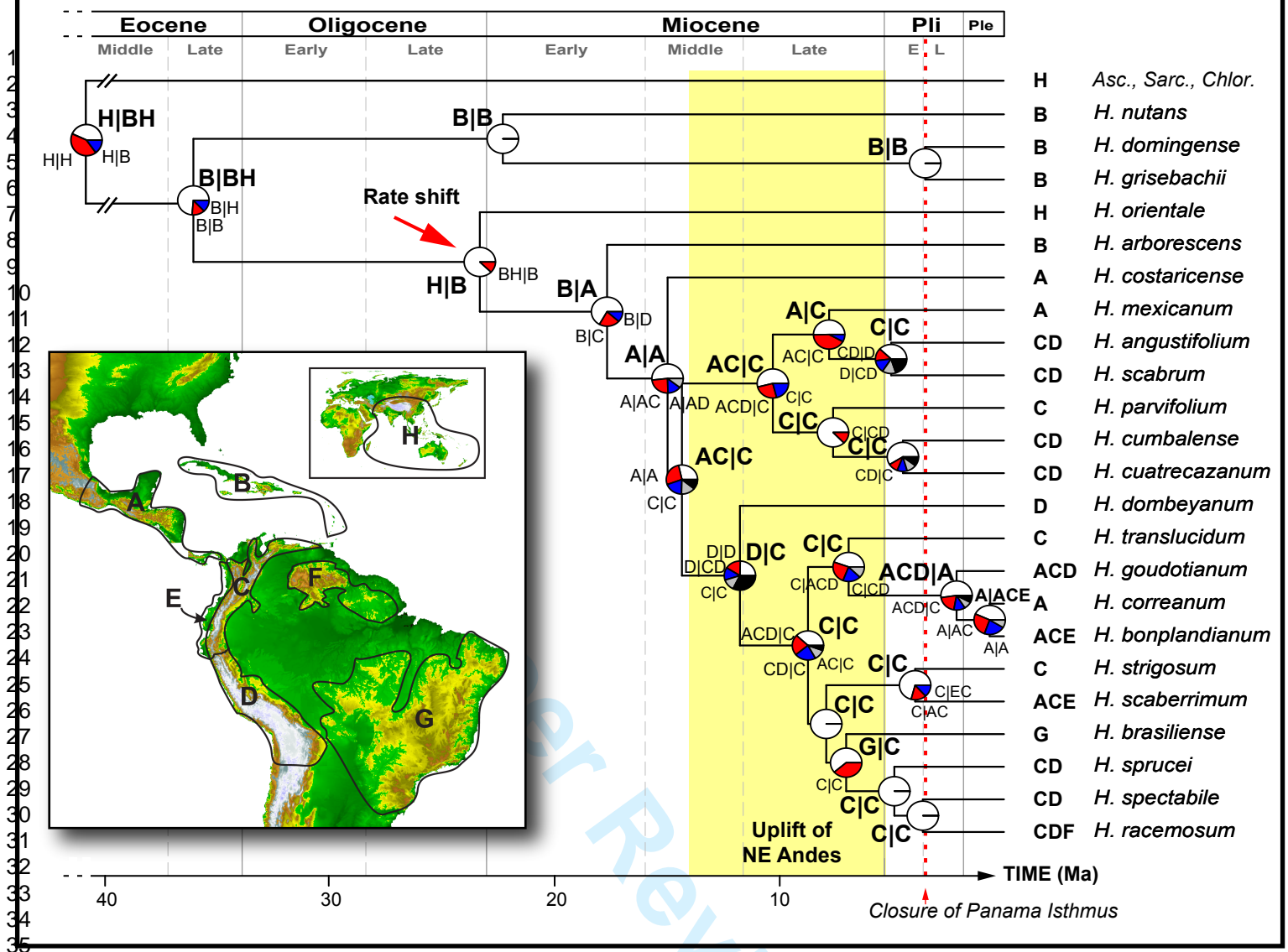
57
58 1142 FIGURE 5. Testing departure of the empirical chronogram of Chloranthaceae (Fig. 2) from a
59
60 1143 constant-rate birth-death diversification model. The thick line represents the lineage through

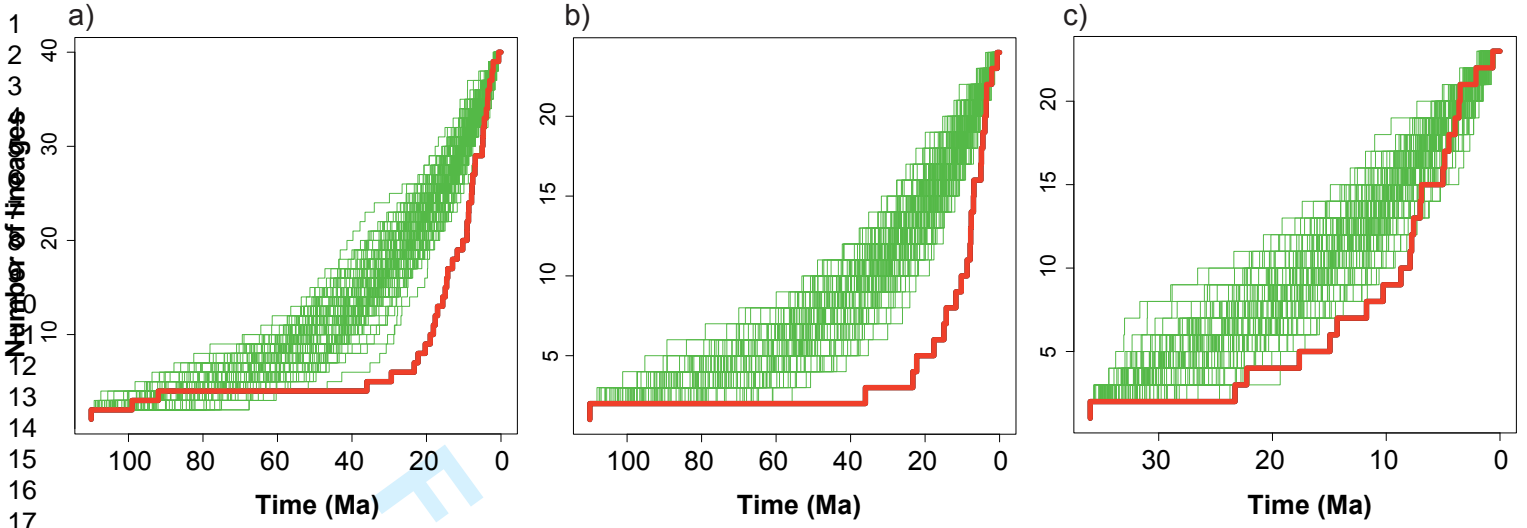
1
2
3 1144 time curve (LTT) for: a) Chloranthaceae, b) the *Hedyosmum* stem lineage, and c) the
4
5 1145 *Hedyosmum* crown group, plotted against LTT curves of 100 phylogenies (thin lines)
6
7
8 1146 simulated under a 2:1 birth-death process using the ML estimate of the speciation rate under
9
10 1147 the pure birth model in LASER (see Table 2). Phylogenies were simulated to each group's
11
12 1148 present diversity and taxa randomly sampled from them to produce a tree with the same
13
14 1149 number of species as the original phylogeny, using the package TreeSim (Stadler 2011).
15
16 1150 Simulated phylogenies were rescaled using the R package APE (Paradis et al. 2004) to have
17
18 1151 their basal divergence coincident with the root age of the observed phylogeny.
19
20 1152
21
22
23
24 1153 FIGURE 6. Testing alternative extinction scenarios to explain the temporal gap between stem
25
26 1154 and crown age in Chloranthaceae (Fig. 2). a) Overlay LTT plots of 100 phylogenies
27
28 1155 simulated under a mass extinction scenario in which there is an early radiation ($b = 0.2$, $d =$
29
30 1156 0.1) followed by an episode of mass extinction at 65 Ma (the K/T event) that extirpates 95%
31
32 1157 of extant lineages, and a second episode of tree growth with high background extinction ($b =$
33
34 1158 0.2 , $d = 0.19$). b) Same as in (a) but with the episode of mass extinction occurring at 35 Ma
35
36 1159 (the Terminal Eocene Event); parameters: $b = 0.19$, $d=0.1$ and $b=0.2$, $d=0.19$ (before and
37
38 1160 after the mass extinction, respectively). c) Overlay LTT plots of 100 phylogenies simulated
39
40 1161 under a model of high relative extinction rates using ML estimated values ($b = 0.082$, $d =$
41
42 1162 0.067 , $a = d/b$ 0.78, Table 2). d) Same as in (c) but the extinction rate is 95% of the estimated
43
44 1163 speciation rate under the Yule model ($b = 0.046$ (Table 2), $d= 0.043$; $a = b/d = 0.95$). For
45
46 1164 each model, the average LTT plot for 100 phylogenies is shown in the inset above; for the
47
48 1165 mass extinction models, the empirical LTT plot is also drawn for comparison. Phylogenies
49
50 1166 were simulated to 65 species, with a fraction of 62% species randomly sampled from the last
51
52 1167 growth episode to mimic incomplete sampling in the Chloranthaceae phylogeny.
53
54
55
56
57
58
59
60











1
2
3
4
5
6
7
8
9
10
11
12
13
14
15
16
17
18
19
20
21
22
23
24
25
26
27
28
29
30
31
32
33
34
35
36
37
38
39
40
41
42
43
44
45
46
47
48
49
50
51
52
53
54
55
56
57
58
59
60

For Peer Review Only

